Air Quality Modeling Technical Support Document for Regulatory Impact Analysis of the Standards of Performance for New, Reconstructed, and Modified Sources and Emissions Guidelines for Existing Sources: Oil and Natural Gas Sector Climate Review

EPA-454/R-23-007
November 2023

Air Quality Modeling Technical Support Document for Regulatory Impact Analysis of the Standards of Performance for New, Reconstructed, and Modified Sources and Emissions Guidelines for Existing Sources: Oil and Natural Gas Sector Climate Review

U.S. Environmental Protection Agency
Office of Air Quality Planning and Standards
Air Quality Assessment Division
Research Triangle Park, NC

Contents

1. Introduction

In this technical support document (TSD) we describe the air quality modeling performed to support EPA's "Regulatory Impact Analysis of the Standards of Performance for New, Reconstructed, and Modified Sources and Emissions Guidelines for Existing Sources: Oil and Natural Gas Sector Climate Review." For this rule, EPA used photochemical modeling to create ozone surfaces[1] that were then used in air pollution health benefits calculations of three regulatory alternatives: the final rule, a less stringent alternative and a more stringent alternative. The modeling-based ozone surfaces are used to quantify ozone impacts resulting from changes to VOC emissions from oil and natural gas sources affected by this rule. As described in this TSD, EPA performed air quality modeling for a 2016 base year and a 2026 future year. Ozone source apportionment modeling was performed for 2026 to characterize the relationship between state-level oil and natural gas-related VOC emissions with ozone concentrations. The 2026 source apportionment modeling was then used to create ozone surfaces for the baseline and regulatory alternatives in each of four years of analysis: 2024, 2027, 2028 and 2038.

The remaining sections of this TSD are as follows. Section 2 describes the air quality modeling platform. Section 3 describes the 2026 source apportionment modeling and the procedures for applying source apportionment modeling and projected emissions changes from the rule to estimate ozone impacts. Section 4 describes the evaluation of 2016 model predictions of 8-hour (hr) daily maximum (MDA8) ozone concentrations using measured (i.e., observed) data. Section 5 describes an assessment conducted to compare source apportionment-based estimated impacts to full-scale air quality modeling for two emissions reduction scenarios relevant to the oil and natural gas sector. Section 6 summarizes uncertainties and limitations of the ozone surface estimates.

2. Air Quality Modeling Platform

The EPA used a 2016-based air quality modeling platform to provide the foundational model-input data sets for 2016 and the future years of analysis. These inputs include emissions for 2016 and 2026 developed for the "2016v2" emissions modeling platform as well as meteorology, initial and boundary condition concentrations, and other inputs representative of the 2016 base year. The 2016v2 emissions modeling platform is described in US EPA (2022a). The meteorological and

[1] "ozone surfaces" refers to continuous gridded spatial fields using a 12 x 12 km resolution grid-cell resolution

initial and boundary condition data used as input to the air quality modeling and the model performance evaluation for MDA8 ozone are described below.

2.1 Air Quality Model Configuration and Model Simulations

The photochemical model simulations performed for this proposed rule used the Comprehensive Air Quality Model with Extensions (CAMx version 7.10, Ramboll, 2021). CAMx is a three-dimensional grid-based Eulerian air quality model designed to simulate the formation and fate of oxidant precursors, primary and secondary particulate matter concentrations, and deposition over regional and urban spatial scales (e.g., the contiguous U.S.). Consideration of the different processes (e.g., transport and deposition) that affect primary (directly emitted) and secondary (formed by atmospheric processes) pollutants at the regional scale in different locations is fundamental to understanding and assessing the effects of emissions on air quality concentrations. For this assessment, EPA used the CAMx Anthropogenic Precursor Culpability Analysis (APCA) technique[2] to model ozone contributions that are then applied to estimate ozone impacts of this final rule as described below in section 3.

The geographic extent of the modeling domains that were used for air quality modeling in this analysis are shown in Figure 2-1. The large outer domain covers the 48 contiguous states along with most of Canada and all of Mexico with a horizontal resolution of 36 x 36 km (i.e., 36 km domain). The inner domain covers the 48 contiguous states along with adjacent portions of Canada and Mexico at 12 x 12 km resolution (i.e., 12 km domain).

[2]As part of this technique, ozone formed from reactions between biogenic VOC and NO_X with anthropogenic NO_X and VOC are assigned to the source of anthropogenic emissions.

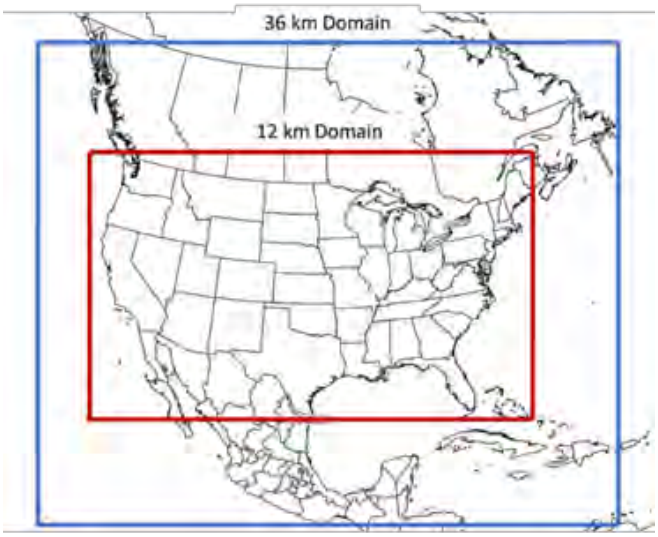

Figure 2-1. Air quality modeling domains.

CAMx requires a variety of input files that contain information pertaining to the modeling domain and simulation period. These include gridded, hourly emissions estimates and meteorological data, and initial and boundary concentrations. Separate emissions inventories were prepared for the 2016 base year and the 2026 future year. All other inputs (i.e., meteorological fields, initial concentrations, ozone column, photolysis rates, and boundary concentrations) were specified for the 2016 base year model application and remained unchanged for the projection-year model simulations.[3]

The 12 km CAMx model simulations performed for this proposed rule are listed in Table 2-1. The simulation period for each run was preceded by a 15-day ramp-up period. Also, the 2026fj oil and natural gas state-sector source apportionment model simulations, 2026fj_oilgassa, were performed for April through September in order to provide sector contribution data that aligns with the April through September average MDA8 concentration, which is the primary health-based metric used to inform the ozone benefits analysis in the RIA.

[3] EPA used the CAMx7.1chemparam.CB6r5_CF2E chemical parameter file for all the CAMx model runs described in this TSD.

Table 2-1. Model run name, case name and simulation period for each model run.

Year	Model Run	Case Name	Simulation Period
2016	2016 baseline	2016fj	Annual
2026	2026 baseline	2026fj	Annual
	2026 state O&G contributions	2026fj_oilgassa	April - September[4]

2.2 Meteorological Data for 2016

This section describes the meteorological modeling that was performed to provide meteorological data for 2016 for input to air quality modeling. The 2016 meteorological data were derived from running Version 3.8 of the Weather Research Forecasting Model (WRF) (Skamarock, et al., 2008). The meteorological outputs from WRF include hourly-varying horizontal wind components (i.e., speed and direction), temperature, moisture, vertical diffusion rates, and rainfall rates for each grid cell in each vertical layer. Selected physics options used in the WRF simulations include Pleim-Xiu land surface model (Xiu and Pleim, 2001; Pleim and Xiu, 2003), Asymmetric Convective Model version 2 planetary boundary layer scheme (Pleim 2007a,b), Kain-Fritsch cumulus parameterization (Kain, 2004) utilizing the moisture-advection trigger (Ma and Tan, 2009), Morrison double moment microphysics (Morrison et al., 2005; Morrison and Gettelman, 2008), and RRTMG longwave and shortwave radiation schemes (Iacono et.al., 2008).

Both the 36 km and 12 km WRF model simulations utilize a Lambert conformal projection centered at (-97,40) with true latitudes of 33 and 45 degrees north. The 36 km domain contains 184 cells in the X direction and 160 cells in the Y direction. The 12 km domain contains 412 cells in the X direction and 372 cells in the Y direction. The atmosphere is resolved with 35 vertical layers up to 50 millibar (see Table 2-2), with the thinnest layers being nearest the surface to better resolve the planetary boundary layer (PBL).

The 36 km WRF model simulation was initialized using the 0.25-degree GFS analysis and 3-hour forecast from the 00 GMT, 06 GMT, 12 GMT, and 18 GMT simulations. The 12 km model was initialized using the 12 km North American Model (12NAM) analysis product provided by National Climatic Data Center (NCDC).[5] The 40 km Eta Data Assimilation System (EDAS) analysis (ds609.2)

[4] Because the model simulations run in Greenwich Mean Time (GMT), the actual simulation period included October 1 in order to obtain MDA8 ozone concentrations based on local time for September 30.

[5] https://www.ncdc.noaa.gov/data-access/model-data/model-datasets/north-american-mesoscale-forecast-system-nam

from the National Center for Atmospheric Research (NCAR) was used where 12NAM data was unavailable.[6] Analysis nudging for temperature, wind, and moisture was applied above the boundary layer only. The model simulations were conducted continuously. The "ipxwrf" program was used to initialize deep soil moisture at the start of the run using a 10-day spin-up period (Gilliam and Pleim, 2010). Land use and land cover data were based on the USGS for the 36NOAM simulation and the 2011 National Land Cover Database (NLCD 2011) for the 12US simulation. Sea surface temperatures were ingested from the Group for High Resolution Sea Surface Temperatures (GHRSST) (Stammer et al., 2003) 1 km SST data. Additionally, lightning data assimilation was utilized to suppress (force) deep convection where lightning is absent (present) in observational data. This method is described by Heath et al. (2016) and was employed to help improve precipitation estimates generated by the model.

Table 2-2. Vertical layers and their approximate height above ground level.

WRF Layer	Height (m)	Pressure (mb)	Sigma
35	17,556	5000	0.000
34	14,780	9750	0.050
33	12,822	14500	0.100
32	11,282	19250	0.150
31	10,002	24000	0.200
30	8,901	28750	0.250
29	7,932	33500	0.300
28	7,064	38250	0.350
27	6,275	43000	0.400
26	5,553	47750	0.450
25	4,885	52500	0.500
24	4,264	57250	0.550
23	3,683	62000	0.600
22	3,136	66750	0.650
21	2,619	71500	0.700
20	2,226	75300	0.740
19	1,941	78150	0.770
18	1,665	81000	0.800
17	1,485	82900	0.820
16	1,308	84800	0.840
15	1,134	86700	0.860
14	964	88600	0.880
13	797	90500	0.900
12	714	91450	0.910

[6] https://www.ready.noaa.gov/edas40.php.

11	632	92400	0.920
10	551	93350	0.930
9	470	94300	0.940
8	390	95250	0.950
7	311	96200	0.960
6	232	97150	0.970
5	154	98100	0.980
4	115	98575	0.985
3	77	99050	0.990
2	38	99525	0.995
1	19	99763	0.9975
Surface	0	100000	1.000

Details of the annual 2016 meteorological model simulation and evaluation are provided in US EPA (2019).

The meteorological data generated by the WRF simulations were processed using wrfcamx v4.7 (Ramboll 2021) meteorological data processing program to create 35-layer gridded model-ready meteorological inputs to CAMx. In running wrfcamx, vertical eddy diffusivities (Kv) were calculated using the Yonsei University (YSU) (Hong et al., 2006) mixing scheme. We used a minimum Kv of 0.1 m^2/sec except for urban grid cells where the minimum Kv was reset to 1.0 m^2/sec within the lowest 200 m of the surface in order to enhance mixing associated with the nighttime "urban heat island" effect. In addition, we invoked the subgrid convection and subgrid stratoform cloud options in our wrfcamx run for 2016.

2.3 Initial and Boundary Concentrations

The lateral boundary and initial species concentrations for the 36 km simulations were derived from outputs of a three-dimensional hemispheric atmospheric chemistry model, the Hemispheric version of the Community Multi-scale Air Quality Model (H-CMAQ) version 3.1.1 which was run for 2016[7]. The H-CMAQ predictions were used to provide one-way dynamic boundary concentrations at one-hour intervals and an initial concentration field for the 36 km CAMx simulations for 2016 and 2023.

[7] More information about the H-CMAQ model and other applications using this tool is available at: https://www.epa.gov/cmaq/hemispheric-scale-applications. Note that EPA used the same initial and boundary conditions for the 2016v2 air quality modeling as was used for the 2016v1 air quality modeling.

Air quality modeling for the 36 km domain was used to provide initial and boundary conditions for the nested 12 km domain model simulations. Both the 36 km and 12 km modeling domains have 35 vertical layers with a top at about 17,550 meters, or 50 millibars (mb). The model simulations produce hourly air quality concentrations for each grid cell across each modeling domain. Modeling for the 36 km domain was performed for 2016 and 2023. Outputs from the 2016 36 km simulation were used to provide initial and boundary conditions for the 2016 12 km model simulation. Outputs from the 2023 36 km simulation were used to provide initial and boundary conditions for the 2026 12 km simulations.

2.5 Air Quality Model Evaluation

An operational model performance evaluation for ozone was conducted to examine the ability of the CAMx modeling system to simulate 2016 measured MDA8 ozone concentrations. This evaluation focused on graphical analyses and statistical metrics of model predictions versus observations. Details on the evaluation methodology, the calculation of performance statistics, and results are provided in Section 4. Overall, the ozone model performance statistics for the CAMx 2016fj simulation are within or close to the ranges found in peer-reviewed applications (e.g., Simon et al, 2012 and Emery et al, 2017). As described in Section 4, the predictions from the 2016v2 modeling platform correspond closely to observed concentrations in terms of the magnitude, temporal fluctuations, and geographic differences for MDA8 ozone. Thus, the model performance results demonstrate the scientific credibility of our 2016v2 modeling platform. These results provide confidence in the ability of the modeling platform to provide a reasonable projection of expected future year ozone concentrations and contributions.

3. Ozone Contribution Modeling and Methodology for Calculating Ozone Impacts of the Final Rule

EPA performed state-by-state[8] ozone source apportionment modeling for oil and natural gas sources using the CAMx APCA technique for the 12 km resolution modeling domain shown in Figure 2-1. This modeling provides data on the ozone contributions from projected 2026 base case VOC emissions from oil and natural gas source types covered by

[8] while we bundle some states and split up TX, we use term "state-by-state" for convenience

this rulemaking in each state. The state-by-state oil and natural gas sector source apportionment modeling is described in Section 3.1. In Section 3.2 we describe the method for approximating the ozone impacts of the regulatory alternatives using these modeling outputs. The basic methodology for determining air quality changes described in Section 3.2 is the same as that used in the RIAs from multiple previous rules (U.S. EPA, 2019b, 2020a, 2020b, 2021, 2023a, 2023b, 2023c, 2023d).

3.1 Description of 2026 State-by-State Oil and Natural Gas Sector Source Apportionment Modeling

In the state-by-state source apportionment model run, we tracked the ozone formed from each of the following contribution categories (i.e., "tags"):

- Oil and Natural Gas State-Level Emissions – anthropogenic NO_X and VOC emissions from oil and natural gas source types covered by this rulemaking[9] tracked individually from each of the contiguous 48 states.[10,11,12] Table 3-3 provides Annual NO_X and VOC emissions associated with each state-level oil and natural gas tag.
- Other[13] – all other emissions in the 12 km domain including biogenic NO_X and VOC emissions domain-wide, combined emissions from wild and prescribed fires, all anthropogenic NO_X and VOC emissions from Canada and Mexico, all US anthropogenic NO_X and VOC emissions that were not included in one of the oil and natural gas state-level tags;
- Initial and Boundary Concentrations – air quality concentrations used to initialize the 12 km model simulation and air quality concentrations transported into the 12 km modeling

[9] Table 3-1 identifies SCCs associated with source types covered by this rulemaking for the purpose of this modeling exercise

[10] No tags were included for the following states that have no emissions from the source types listed in Table 3-1: CT, DE, GA, IA, MA, ME, MN, NC, NH, RI, VT, WI,WA

[11] Oil and gas emissions from the state of TX were split into 3 separate sub-state regional tags as described in Table 3-2

[12] States with less than 100 tpy of VOC emissions from the source types listed in Table 3-1 were combined into multi-state tags as shown in Table 3-3

[13] Ozone contributions from separate tags tracking biogenic emissions, fire emissions, Canadian and Mexican anthropogenic emissions combined, offshore emissions, and state-by-state total anthropogenic emissions are available for the 2026fj case from modeling conducted to support the Federal Implementation Plan Addressing Regional Ozone Transport for the 2015 Ozone National Ambient Air Quality Standards Proposed Rulemaking and are available in the docket for that rulemaking.

domain from the lateral boundaries

The tagged sources account for all ozone sources simulated by the model such that the sum of tagged ozone contributions adds to the total modeled ozone at each hour and grid cell.

Table 3-1. List of Oil and Natural Gas Source Types Tracked in the State-Level Oil and Natural Gas Tags

Source Classification Code (SCC)	Description
31000101	Industrial Processes;Oil and Gas Production;Crude Oil Production;Well Completion;
31000130	Industrial Processes;Oil and Gas Production;Crude Oil Production;Fugitives: Compressor Seals;
31000132	Industrial Processes;Oil and Gas Production;Crude Oil Production;Atmospheric Wash Tank (2nd Stage of Gas-Oil Separation): Flashing Loss;
31000133	Industrial Processes;Oil and Gas Production;Crude Oil Production;Storage Tank;
31000151	Industrial Processes;Oil and Gas Production;Crude Oil Production;Pneumatic Controllers, Low Bleed;
31000152	Industrial Processes;Oil and Gas Production;Crude Oil Production;Pneumatic Controllers High Bleed >6 scfh;
31000153	Industrial Processes;Oil and Gas Production;Crude Oil Production;Pneumatic Controllers Intermittent Bleed;
31000207	Industrial Processes;Oil and Gas Production;Natural Gas Production;Valves: Fugitive Emissions;
31000212	Industrial Processes;Oil and Gas Production;Natural Gas Production;Condensate Storage Tank;
31000213	Industrial Processes;Oil and Gas Production;Natural Gas Production;Produced Water Storage Tank;
31000214	Industrial Processes;Oil and Gas Production;Natural Gas Production;Natural Gas Liquids Storage Tank;
31000220	Industrial Processes;Oil and Gas Production;Natural Gas Production;All Equipt Leak Fugitives (Valves, Flanges, Connections, Seals, Drains;
31000225	Industrial Processes;Oil and Gas Production;Natural Gas Production;Compressor Seals;
31000231	Industrial Processes;Oil and Gas Production;Natural Gas Production;Fugitives: Drains;
31000233	Industrial Processes;Oil and Gas Production;Natural Gas Production;Pneumatic Controllers, Low Bleed;
31000235	Industrial Processes;Oil and Gas Production;Natural Gas Production;Pneumatic Controllers Intermittent Bleed;

31000309	Industrial Processes;Oil and Gas Production;Natural Gas Processing;Compressor Seals;
31000324	Industrial Processes;Oil and Gas Production;Natural Gas Processing;Pneumatic Controllers Low Bleed;
31000325	Industrial Processes;Oil and Gas Production;Natural Gas Processing;Pneumatic Controllers, High Bleed >6 scfh;
31000326	Industrial Processes;Oil and Gas Production;Natural Gas Processing;Pneumatic Controllers Intermittent Bleed;
31088811	Industrial Processes;Oil and Gas Production;Fugitive Emissions;Fugitive Emissions;
2310010200	Industrial Processes;Oil and Gas Exploration and Production;Crude Petroleum;Oil Well Tanks - Flashing & Standing/Working/Breathing
2310010300	Industrial Processes;Oil and Gas Exploration and Production;Crude Petroleum;Oil Well Pneumatic Devices
2310010700	Industrial Processes;Oil and Gas Exploration and Production;Crude Petroleum;Oil Well Fugitives
2310011020	Industrial Processes;Oil and Gas Exploration and Production;On-Shore Oil Production;Storage Tanks: Crude Oil
2310011500	Industrial Processes;Oil and Gas Exploration and Production;On-Shore Oil Production;Fugitives: All Processes
2310011501	Industrial Processes;Oil and Gas Exploration and Production;On-Shore Oil Production;Fugitives: Connectors
2310011502	Industrial Processes;Oil and Gas Exploration and Production;On-Shore Oil Production;Fugitives: Flanges
2310011503	Industrial Processes;Oil and Gas Exploration and Production;On-Shore Oil Production;Fugitives: Open Ended Lines
2310011504	Industrial Processes;Oil and Gas Exploration and Production;On-Shore Oil Production;Fugitives: Pumps
2310011505	Industrial Processes;Oil and Gas Exploration and Production;On-Shore Oil Production;Fugitives: Valves
2310011506	Industrial Processes;Oil and Gas Exploration and Production;On-Shore Oil Production;Fugitives: Other
2310021010	Industrial Processes;Oil and Gas Exploration and Production;On-Shore Gas Production;Storage Tanks: Condensate
2310021300	Industrial Processes;Oil and Gas Exploration and Production;On-Shore Gas Production;Gas Well Pneumatic Devices
2310021310	Industrial Processes;Oil and Gas Exploration and Production;On-Shore Gas Production;Gas Well Pneumatic Pumps
2310021500	Industrial Processes;Oil and Gas Exploration and Production;On-Shore Gas Production;Gas Well Completion – Flaring
2310021501	Industrial Processes;Oil and Gas Exploration and Production;On-Shore Gas Production;Fugitives: Connectors
2310021502	Industrial Processes;Oil and Gas Exploration and Production;On-Shore Gas Production;Fugitives: Flanges
2310021503	Industrial Processes;Oil and Gas Exploration and Production;On-Shore Gas Production;Fugitives: Open Ended Lines

2310021504	Industrial Processes;Oil and Gas Exploration and Production;On-Shore Gas Production;Fugitives: Pumps
2310021505	Industrial Processes;Oil and Gas Exploration and Production;On-Shore Gas Production;Fugitives: Valves
2310021506	Industrial Processes;Oil and Gas Exploration and Production;On-Shore Gas Production;Fugitives: Other
2310021509	Industrial Processes;Oil and Gas Exploration and Production;On-Shore Gas Production;Fugitives: All Processes
2310021602	Industrial Processes;Oil and Gas Exploration and Production;On-Shore Gas Production;Gas Well Venting – Recompletions
2310021603	Industrial Processes;Oil and Gas Exploration and Production;On-Shore Gas Production;Gas Well Venting – Blowdowns
2310023010	Industrial Processes;Oil and Gas Exploration and Production;Coal Bed Methane Natural Gas;Storage Tanks: Condensate
2310023300	Industrial Processes;Oil and Gas Exploration and Production;Coal Bed Methane Natural Gas;Pneumatic Devices
2310023310	Industrial Processes;Oil and Gas Exploration and Production;Coal Bed Methane Natural Gas;Pneumatic Pumps
2310023509	Industrial Processes;Oil and Gas Exploration and Production;Coal Bed Methane Natural Gas;Fugitives
2310023511	Industrial Processes;Oil and Gas Exploration and Production;Coal Bed Methane Natural Gas;Fugitives: Connectors
2310023512	Industrial Processes;Oil and Gas Exploration and Production;Coal Bed Methane Natural Gas;Fugitives: Flanges
2310023513	Industrial Processes;Oil and Gas Exploration and Production;Coal Bed Methane Natural Gas;Fugitives: Open Ended Lines
2310023515	Industrial Processes;Oil and Gas Exploration and Production;Coal Bed Methane Natural Gas;Fugitives: Valves
2310023516	Industrial Processes;Oil and Gas Exploration and Production;Coal Bed Methane Natural Gas;Fugitives: Other
2310023600	Industrial Processes;Oil and Gas Exploration and Production;Coal Bed Methane Natural Gas;CBM Well Completion: All Processes
2310023603	Industrial Processes;Oil and Gas Exploration and Production;Coal Bed Methane Natural Gas;CBM Well Venting – Blowdowns
2310030220	Industrial Processes;Oil and Gas Exploration and Production;Natural Gas Liquids;Gas Well Tanks - Flashing & Standing/Working/Breathing, Controlled
2310030300	Industrial Processes;Oil and Gas Exploration and Production;Natural Gas Liquids;Gas Well Water Tank Losses
2310111401	Industrial Processes;Oil and Gas Exploration and Production;On-Shore Oil Exploration;Oil Well Pneumatic Pumps
2310111700	Industrial Processes;Oil and Gas Exploration and Production;On-Shore Oil Exploration;Oil Well Completion: All Processes
2310111701	Industrial Processes;Oil and Gas Exploration and Production;On-Shore Oil Exploration;Oil Well Completion: Flaring
2310121401	Industrial Processes;Oil and Gas Exploration and Production;On-Shore Gas Exploration;Gas Well Pneumatic Pumps

2310121700	Industrial Processes;Oil and Gas Exploration and Production;On-Shore Gas Exploration;Gas Well Completion: All Processes
2310321010	Industrial Processes;Oil and Gas Exploration and Production;On-Shore Gas Production - Conventional;Storage Tanks: Condensate
2310321603	Industrial Processes;Oil and Gas Exploration and Production;On-Shore Gas Production - Conventional;Gas Well Venting – Blowdowns
2310421010	Industrial Processes;Oil and Gas Exploration and Production;On-Shore Gas Production - Unconventional;Storage Tanks: Condensate
2310421603	Industrial Processes;Oil and Gas Exploration and Production;On-Shore Gas Production - Unconventional;Gas Well Venting – Blowdowns

Table 3-2. List of Counties Included in Each Texas Sub-Regional Tag

Texas Sub-Region Name	**Subpart W Basins**	**Counties**
Gulf	Eagle Ford, Western Gulf	Aransas, Atascosa, Austin, Bastrop, Bee, Brazoria, Brazos, Brooks, Burleson, Caldwell, Calhoun, Cameron, Chambers, Colorado, DeWitt, Dimmit, Duval, Fayette, Fort Bend, Frio, Galveston, Goliad, Gonzales, Grimes, Guadalupe, Hardin, Harris, Hidalgo, Jackson, Jasper, Jefferson, Jim Hogg, Jim Wells, Karnes, Kenedy, Kleberg, La Salle, Lavaca, Lee, Liberty, Live Oak, Madison, Matagorda, Maverick, McMullen, Milam, Montgomery, Newton, Nueces, Orange, Polk, Refugio, San Jacinto, San Patricio, Starr, Trinity, Tyler, Victoria, Walker, Waller, Washington, Webb, Wharton, Willacy, Wilson, Zapata, Zavala
Central	Bend Arch-Fort Worth Basin, East Texas Basin, Western Gulf	Anderson, Angelina, Archer, Bandera, Baylor, Bell, Bexar, Blanco, Bosque, Bowie, Brown, Burnet, Callahan, Camp, Cass, Cherokee, Clay, Coleman, Collin, Comal, Comanche, Cooke, Coryell, Dallas, Delta, Denton, Eastland, Ellis, Erath, Falls, Fannin, Franklin, Freestone, Gillespie, Grayson, Gregg, Hamilton, Harrison, Hays, Henderson, Hill, Hood, Hopkins, Houston, Hunt, Jack, Johnson, Kaufman, Kendall, Kerr, Kinney, Lamar, Lampasas, Leon, Limestone, Llano, Marion, Mason, McCulloch, McLennan, Medina, Mills, Montague, Morris, Nacogdoches, Navarro, Palo Pinto, Panola, Parker, Rains, Real, Red River, Robertson, Rockwall, Rusk, Sabine, San Augustine, San Saba, Shackelford, Shelby, Smith, Somervell, Stephens, Tarrant, Throckmorton, Titus, Travis, Upshur, Uvalde, Van Zandt, Williamson, Wise, Wood, Young
Western	Anadarko Basin, Bend Arch-Fort	Andrews, Armstrong, Bailey, Borden, Brewster, Briscoe, Carson, Castro, Childress, Cochran, Coke, Collingsworth, Concho, Cottle, Crane, Crockett, Crosby, Culberson, Dallam, Dawson, Deaf Smith, Dickens, Donley, Ector,

	Worth Basin, Marathon Thrust Belt, Palo Duro Basin, Permian Basin	Edwards, El Paso, Fisher, Floyd, Foard, Gaines, Garza, Glasscock, Gray, Hale, Hall, Hansford, Hardeman, Hartley, Haskell, Hemphill, Hockley, Howard, Hudspeth, Hutchinson, Irion, Jeff Davis, Jones, Kent, Kimble, King, Knox, Lamb, Lipscomb, Loving, Lubbock, Lynn, Martin, Menard, Midland, Mitchell, Moore, Motley, Nolan, Ochiltree, Oldham, Parmer, Pecos, Potter, Presidio, Randall, Reagan, Reeves, Roberts, Runnels, Schleicher, Scurry, Sherman, Sterling, Stonewall, Sutton, Swisher, Taylor, Terrell, Terry, Tom Green, Upton, Val Verde, Ward, Wheeler, Wichita, Wilbarger, Winkler, Yoakum

Table 3-3. Annual Emissions Associated with Each Oil and Natural Gas Tag

O&G Tag Description	NO_X (tons)	VOC (tons)
Alabama	6	8,596
Arizona	0	163
Arkansas	2	4,646
California	0	850
Colorado	353	55,627
Florida	1	403
ID+MT+OR	90	22,334
Illinois	12	50,174
Indiana	2	10,143
Kansas	29	65,092
Kentucky	4	32,649
Louisiana	90	49,586
MD+VA	1	6,439
Michigan	2	13,303
Mississippi	9	7,263
Missouri	0	841
Nebraska	0	1,843
Nevada	0	108
New Mexico	395	143,531
NJ+NY	2	4,624
North Dakota	3,872	72,735
Offshore	0	13,274
Ohio	63	13,827
Oklahoma	1,908	152,213
Pennsylvania	6,795	119,472
SC+TN	1	1,389
South Dakota	7	2,187
Texas Central	77	127,927
Texas Gulf	2,019	336,071
Texas West	1,509	441,349

Utah	4	31,406
West Virginia	168	125,475
Wyoming	1,063	47,726

The source apportionment modeling provided contributions to ozone from anthropogenic NO_X and VOC oil and natural gas emissions in each tag, individually, to ozone concentrations in each model grid cell within the 12 km domain. Examples of the magnitude and spatial extent of tagged ozone contributions are provided in Figure 3-1 through Figure 3-3 for oil and natural gas VOC emissions in ten states. These figures show how the magnitude and the spatial patterns of contributions of oil and natural gas VOC emissions to ozone depend on multiple factors including the magnitude and location of emissions as well as the atmospheric conditions that influence the formation and transport of ozone. For instance, the magnitude of tagged oil and natural gas VOC emissions are similar in Wyoming and Colorado, but ozone impacts from these emissions are much larger in Colorado than Wyoming (Figure 3-1) due to much larger urban NO_x emissions near oil and natural gas sources in Colorado that can react with the oil and natural gas VOC emissions to form ozone in the atmosphere. In New Mexico, the spatial extent of the ozone impacts reflect oil and natural gas VOC emissions locations in two distinct regions of the state (Figure 3-1). In Figure 3-2 it is apparent that the spatial extent of ozone contributions from the three Texas sub-regional tags are distinct and impacted both by the location of the emissions within those sub-regions and by prevailing winds which transport ozone into nearby states. The magnitude of the ozone impact is larger from emissions in the Texas West tag and the Texas Gulf tag than from emissions in the Texas Central tag which is consistent with substantially larger oil and natural gas VOC emissions levels in those to subregions than the Texas Central subregion (Table 3-3).

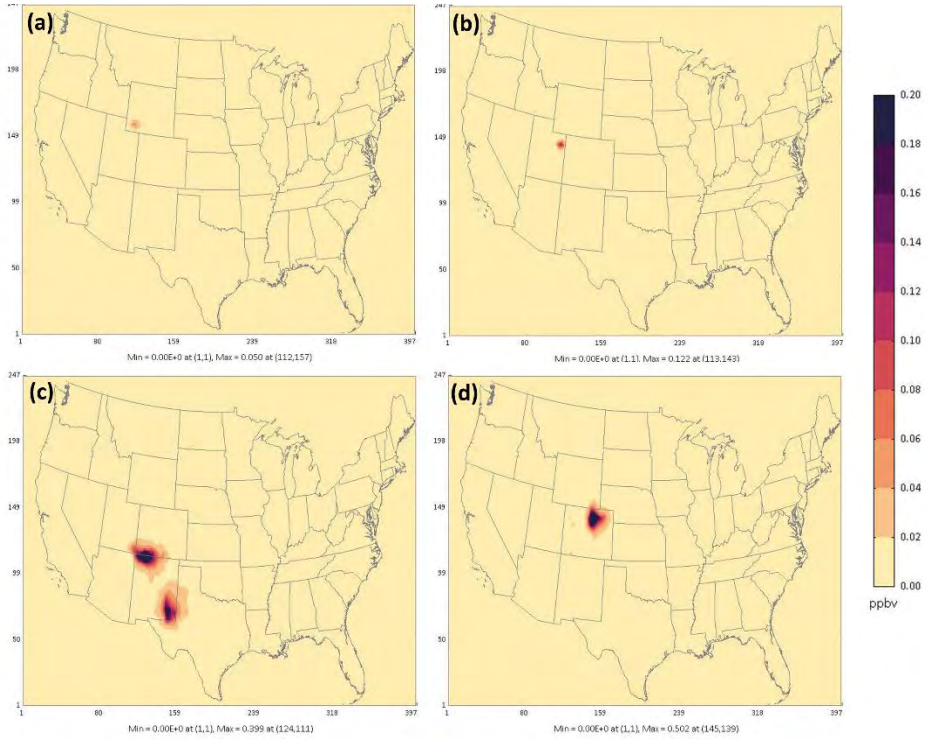

Figure 3-1. Map of April-September Mean MDA8 ozone contributions (ppb) from tagged oil and natural gas VOC emissions located in (a) Wyoming, (b) Utah, (c) New Mexico and (d) Colorado.

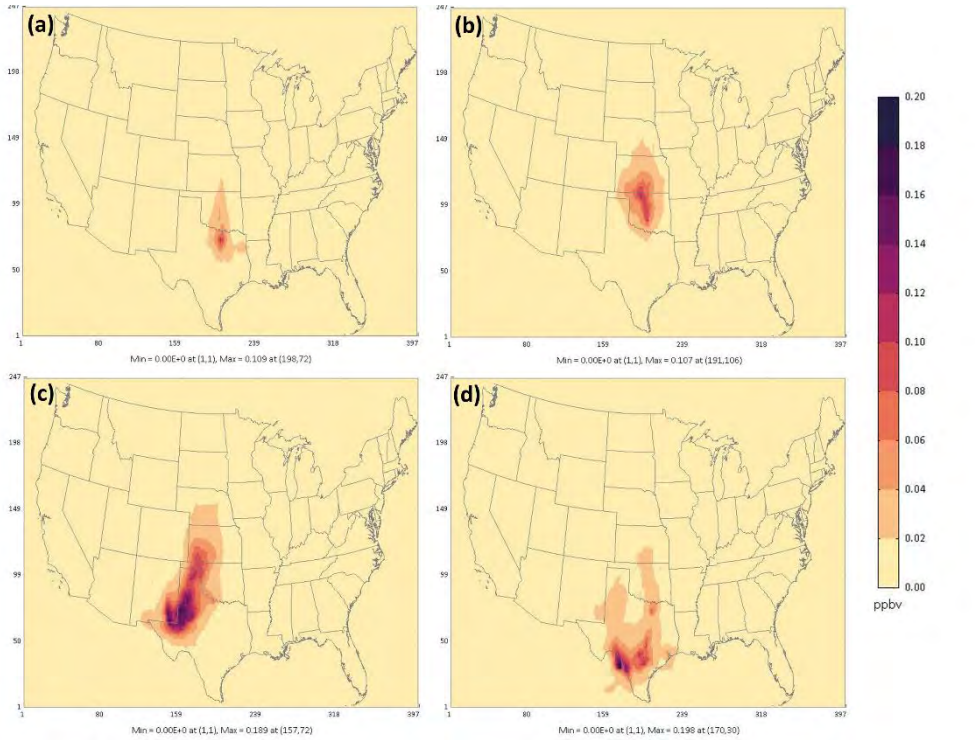

Figure 3-2. Map of April-September Mean MDA8 ozone contributions (ppb) from tagged oil and natural gas VOC emissions located in (a) Texas Central, (b) Oklahoma, (c) Texas West and (d) Texas Gulf.

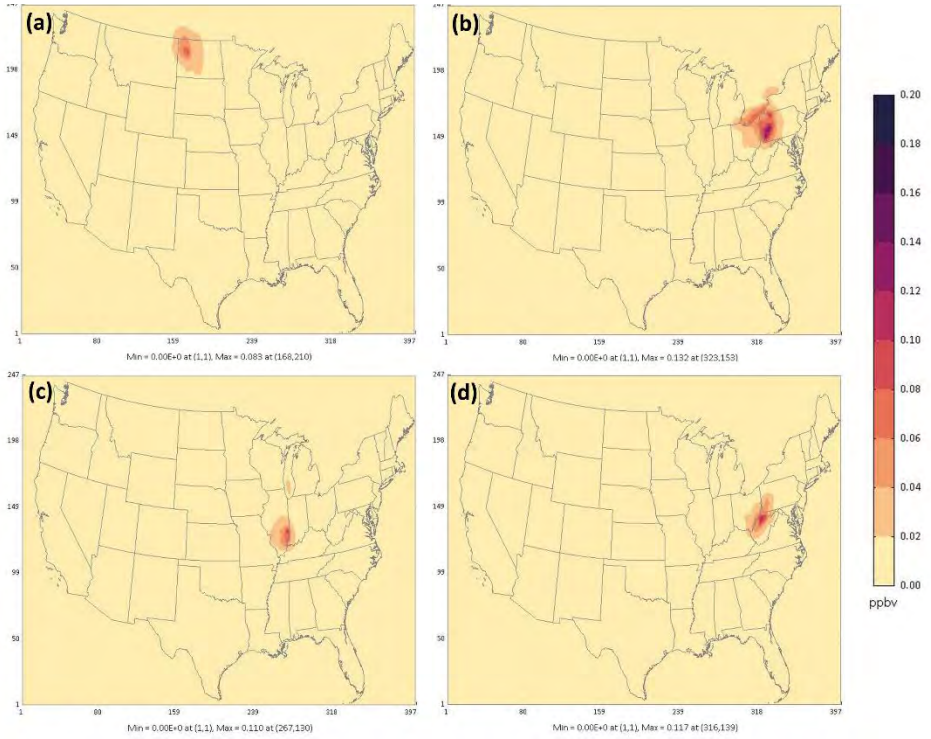

Figure 3-3. Map of April-September Mean MDA8 ozone contributions (ppb) from tagged oil and natural gas VOC emissions located in (a) North Dakota, (b) Pennsylvania, (c) Illinois and (d) West Virginia.

3.2 Source Apportionment Scaling Method for Calculating the Ozone Impacts of the Final Rule

In this section we describe the method for creating spatial fields of the April-September mean of MDA8 ozone (AS-MO3) for baseline and regulatory alternatives based on the 2016 and 2026 modeling. The foundational data include (1) ozone concentrations in each model grid cell from the 2016 and 2026 modeling, (2) ozone contributions in 2026 of oil and natural gas emissions from each state in each model grid cell,[14] (3) 2026 emissions from covered oil and natural gas sources that were used as inputs to the contribution modeling (Table 3-3) and (4) the oil and natural gas emissions for baseline and regulatory alternatives in each state and year of analysis. The development of state-level emissions for the baseline and regulatory alternatives are described in Section 2.2 of US EPA, 2023e. The method to create spatial fields applies scaling factors to gridded source apportionment

[14] Contributions from oil and natural gas sources were modeled using projected emissions for 2026. The resulting contributions were used to construct spatial fields in 2024, 2027, 2028 and 2038.

contributions based on emissions changes between 2026 modeled levels and the baseline and regulatory alternatives. This method is described in detail below.

Spatial fields of ozone for 2026 modeled conditions were created based on "fusing" modeled data with measured concentrations at air quality monitoring locations. To create the spatial fields for each future emissions scenario these fused 2026 model fields are used in combination with 2026 state-by-state oil and natural gas source apportionment modeling and the oil and natural gas emissions for each scenario and year of analysis. Contributions from each state-level oil and natural gas contribution "tag" were scaled based on the ratio of emissions in the year/scenario being evaluated to the emissions in the modeled 2026 scenario. Contributions from tags representing sources other than oil and natural gas are held constant at 2026 levels for each of the scenarios and year. For each scenario and year analyzed, the scaled contributions from all sources were summed together to create a gridded surface of total modeled ozone. The process is described in a step-by-step manner below starting with the methodology for creating AS-MO3 spatial fields.

1. Create fused spatial fields of 2026 AS-MO3 incorporating information from the air quality modeling and from ambient measured monitoring data. The enhanced Voronoi Neighbor Average (eVNA) technique (Ding et al., 2016; Gold et al., 1997; U.S. EPA, 2007) was applied to ozone model predictions in conjunction with measured data to create modeled/measured fused surfaces that leverage measured concentrations at air quality monitor locations and model predictions at locations with no monitoring data.

    1.1. The AS-MO3 eVNA spatial fields are created for the 2016 base year with EPA's software package, Software for the Modeled Attainment Test – Community Edition (SMAT-CE)[15] (U.S. EPA, 2022b) using three years of monitoring data (2015-2017) and the 2016 modeled data.

    1.2. The model-predicted spatial fields (i.e., not the eVNA fields) of AS-MO3 in 2016 were paired with the corresponding model-predicted spatial fields in 2026 to calculate the ratio of AS-MO3 between 2016 and 2026 in each model grid cell.

    1.3. To create a gridded 2026 eVNA surfaces, the spatial fields of 2016/2026 ratios created in step 1.2 were multiplied by the corresponding eVNA spatial fields for 2016 created in step 1.1 to produce an eVNA AS-MO3 spatial field for 2026 using (Eq-1).

[15] SMAT-CE available for download at https://www.epa.gov/scram/photochemical-modeling-tools.

$$\mathrm{eVNA}_{g,2026} = \left(\mathrm{eVNA}_{g,2016}\right) \times \frac{\mathrm{Model}_{g,2026}}{\mathrm{Model}_{g,2016}} \quad \text{Eq-1}$$

- $\mathrm{eVNA}_{g,2026}$ is the eVNA concentration of AS-MO3 in grid-cell, g, in the 2026 future year
- $\mathrm{eVNA}_{g,2016}$ is the eVNA concentration of AS-MO3 in grid-cell, g, in 2016
- $\mathrm{Model}_{g,2026}$ is the CAMx modeled concentration of AS-MO3 in grid-cell, g, in the 2026 future year
- $\mathrm{Model}_{g,2016}$ is the CAMx modeled concentration of AS-MO3 in grid-cell, g, in 2016

2. Create gridded spatial fields of total oil and natural gas AS-MO3 contributions for each combination of scenario and year evaluated.

   2.1. Use the oil and natural gas VOC emissions for the 2024 baseline and the corresponding 2026 modeled oil and natural gas VOC emissions (Table 3-3) to calculate the ratio of 2024 baseline emissions to 2026 modeled emissions for each oil and natural gas state contribution tag (i.e., an ozone scaling factor calculated for each state). These scaling factors are provided in Table 3-4.

   2.2. Calculate adjusted gridded AS-MO3 oil and natural gas contributions that reflect differences in state-oil and natural gas VOC emissions between 2026 and the 2024 baseline by multiplying the VOC scaling factors by the corresponding gridded AS-MO3 ozone contributions[16] from each state-by-state oil and natural gas tag.

   2.3. Add together the adjusted AS-MO3 contributions for each oil and natural gas-state tag to produce spatial fields of adjusted oil and natural gas totals for the 2024 baseline.[17]

   2.4. Repeat steps 2.1 through 2.3 for all 2024 regulatory alternatives (i.e. the final rule scenario, the less stringent alternative, and the more stringent alternative) and for the baseline and regulatory alternatives for each additional year of analysis. All scaling factors for the baseline scenario and the regulatory alternatives are provided in Tables 3-4 through 3-7.

[16] The source apportionment modeling provided separate ozone contributions for ozone formed in VOC-limited chemical regimes (O3V) and ozone formed in NO_X-limited chemical regimes (O3N). The VOC emissions scaling factors are multiplied by the corresponding O3V gridded contributions to MDA8 concentrations. Since there are no predicted changes in NO_X emissions in the control scenarios, the O3N contributions remain unchanged.

[17] The contributions from the unaltered O3N tags are added to the summed adjusted O3V oil and natural gas tags.

3. Create a gridded spatial field of AS-MO3 associated with oil and natural gas VOC emissions for the 2024 baseline by combining the oil and natural gas AS-MO3 contributions from step 2.3 with the corresponding contributions to AS-MO3 from all other sources. Repeat for each of the oil and natural gas contributions created in step 2.4 to create separate gridded spatial fields for the baseline and regulatory alternatives for all other years of analysis.

Steps 2 and 3 in combination can be represented by equation 2:

$$\text{AS-MO3}_{g,i,y} = \text{eVNA}_{g,2026} \times \left(\frac{C_{g,BC}}{C_{g,Tot}} + \frac{C_{g,other}}{C_{g,Tot}} + \sum_{t=1}^{T} \frac{C_{O\&GNOx,g,t}}{C_{g,Tot}} + \sum_{t=1}^{T} \frac{C_{O\&GVOC,g,t}\, S_{VOC,t,i,y}}{C_{g,Tot}} \right) \quad \text{Eq-2}$$

- $\text{AS-MO3}_{g,i,y}$ is the estimated fused model-obs AS-MO3 for grid-cell, "g," scenario, "i,"[18] and year, "y;"[19]
- $\text{eVNA}_{g,2026}$ is the 2026 eVNA AS-MO3 concentration for grid-cell "g" calculated using Eq-1.
- $C_{g,Tot}$ is the total modeled AS-MO3 for grid-cell "g" from all sources in the 2026 source apportionment modeling
- $C_{g,BC}$ is the 2026 AS-MO3 modeled contribution from the modeled boundary inflow;
- $C_{g,other}$ is the 2026 AS-MO3 modeled contribution from all natural and anthropogenic emissions within the modeling domain other than those from oil and natural gas sources;
- $C_{O\&GVOC,g,t}$ is the 2026 AS-MO3 modeled contribution from oil and natural gas emissions of VOCs from state, "t";
- $C_{O\&GNOx,g,t}$ is the 2026 AS-MO3 modeled contribution from oil and natural gas emissions of NO_X from state, "t"; and
- $S_{VOC,t,i,y}$ is the oil and natural gas VOC scaling factor for state, "t," scenario, "i," and year, "y."

[18] Scenario "i" can represent the baseline scenario, the final rule scenario, the less stringent alternative or the more stringent alternative

[19] Year "y" can represent 2024, 2027, 2028 or 2038

Table 3-4. 2024 ozone scaling factors for oil and natural gas tags in the baseline and regulatory alternatives based on ratios of VOC emissions in those scenarios to the 2026 modeled scenario for each state-by-state oil and natural gas tag.

State	Baseline	Less Stringent Alternative	More Stringent Alternative	Final Rule
AL	1.52	1.51	1.51	1.51
AR	4.38	4.35	4.35	4.35
AZ	1.43	1.43	1.43	1.43
CA	7.11	7.11	7.11	7.11
CO	2.68	2.68	2.68	2.68
FL	1.02	1.02	1.02	1.02
IL	0.01	0.01	0.01	0.01
IN	0.03	0.03	0.03	0.03
KS	1.73	1.71	1.71	1.71
KY	0.60	0.59	0.59	0.59
LA	1.61	1.58	1.57	1.57
MI	1.26	1.25	1.25	1.25
MO	0.24	0.24	0.24	0.24
MS	2.77	2.68	2.68	2.68
MT+ID+WA+OR	1.57	1.56	1.56	1.56
ND	2.61	2.56	2.56	2.56
NE+IA	2.60	2.54	2.54	2.54
NY+NJ+CT+RI+MA+VT+NH+ME	2.19	2.17	2.17	2.17
NM	1.49	1.44	1.44	1.44
NV	6.38	6.38	6.38	6.38
OFFSHR	1.00	1.00	1.00	1.00
OH	3.58	3.46	3.46	3.46
OK	1.89	1.83	1.83	1.83
PA	0.78	0.75	0.75	0.75
SD-MN-WI	0.84	0.84	0.84	0.84
TN+GA+NC+SC	0.28	0.28	0.28	0.28
TXG	0.84	0.82	0.82	0.82
TXN	0.84	0.82	0.82	0.82
TXW	1.77	1.69	1.69	1.69
UT	1.06	1.04	1.04	1.04
VA+MD+DE	1.34	1.32	1.32	1.32
WV	0.52	0.52	0.52	0.52
WY	2.77	2.73	2.73	2.73

[1]Texas Gulf and Texas Central VOC emissions were based on estimates of VOC emissions in the Gulf Coast NEMS region within Texas. The proportion of those emissions allocated to the Texas Gulf tag versus the Texas Central tag is based on the relative VOC emissions magnitudes within each of the 2026 tags such that 72.4% of the VOC emissions from the Gulf Coast NEMS were allocated to the Texas Gulf tag and 27.6% of the VOC emissions from the Gulf Coast NEMS were allocated to the Texas Central Tag.

[2]VOC emissions in the Texas West region is the sum of estimated VOC emissions in the Texas Midcontinent NEMS region and the Texas Southwest NEMS region.

Table 3-5. 2027 year ozone scaling factors for oil and natural gas tags in the baseline and regulatory alternatives based on ratios of VOC emissions in those scenarios to the 2026 modeled scenario for each state-by-state oil and natural gas tag.

State	Baseline	Less Stringent Alternative	More Stringent Alternative	Final Rule
AL	1.35	1.32	1.32	1.32
AR	3.96	3.84	3.84	3.84
AZ	1.40	1.37	1.37	1.37
CA	6.45	6.45	6.45	6.45
CO	2.70	2.70	2.70	2.70
FL	1.01	1.00	1.00	1.00
IL	0.01	0.01	0.01	0.01
IN	0.03	0.03	0.03	0.03
KS	1.44	1.36	1.35	1.35
KY	0.54	0.52	0.51	0.51
LA	1.48	1.34	1.34	1.34
MI	1.06	1.04	1.04	1.04
MO	0.21	0.20	0.20	0.20
MS	2.35	2.07	2.07	2.07
MT+ID+WA+OR	1.32	1.29	1.29	1.29
ND	2.66	2.47	2.47	2.47
NE+IA	2.15	1.93	1.92	1.92
NY+NJ+CT+RI+MA+VT+NH+ME	2.00	1.93	1.92	1.92
NM	1.53	1.39	1.39	1.39
NV	4.47	4.47	4.47	4.47
OFFSHR	1.00	1.00	1.00	1.00
OH	3.51	3.12	3.12	3.12
OK	1.89	1.65	1.65	1.65
PA	0.75	0.67	0.66	0.66
SD-MN-WI	0.68	0.65	0.65	0.65
TN+GA+NC+SC	0.28	0.28	0.28	0.28
TXG	0.88	0.80	0.80	0.80
TXN	0.88	0.80	0.80	0.80
TXW	1.86	1.61	1.60	1.60
UT	0.97	0.89	0.89	0.89
VA+MD+DE	1.30	1.24	1.22	1.22
WV	0.50	0.47	0.47	0.47
WY	2.63	2.46	2.45	2.45

[1]Texas Gulf and Texas Central VOC emissions were based on estimates of VOC emissions in the Gulf Coast NEMS region within Texas. The proportion of those emissions allocated to the Texas Gulf tag versus the Texas Central tag is based on the relative VOC emissions magnitudes within each of the 2026 tags such that 72.4% of the VOC emissions from the Gulf Coast NEMS were allocated to the Texas Gulf tag and 27.6% of the VOC emissions from the Gulf Coast NEMS were allocated to the Texas Central Tag.

[2]VOC emissions in the Texas West region is the sum of estimated VOC emissions in the Texas Midcontinent NEMS region and the Texas Southwest NEMS region.

Table 3-6. 2028 year ozone scaling factors for oil and natural gas tags in the baseline and regulatory alternatives based on ratios of VOC emissions in those scenarios to the 2026 modeled scenario for each state-by-state oil and natural gas tag.

State	Baseline	Less Stringent Alternative	More Stringent Alternative	Final Rule
AL	1.29	0.47	0.31	0.32
AR	3.85	1.24	0.82	0.86
AZ	1.38	0.35	0.32	0.32
CA	2.00	1.95	1.89	1.89
CO	1.72	1.72	1.63	1.64
FL	1.11	0.62	0.59	0.60
IL	0.01	0.00	0.00	0.00
IN	0.03	0.01	0.01	0.01
KS	1.37	0.68	0.49	0.50
KY	0.52	0.20	0.11	0.12
LA	1.45	0.56	0.45	0.46
MI	1.00	0.49	0.31	0.32
MO	0.20	0.09	0.08	0.08
MS	2.25	1.20	1.13	1.13
MT+ID+WA+OR	1.27	0.84	0.75	0.75
ND	3.03	2.43	2.39	2.39
NE+IA	2.04	1.15	1.00	1.01
NY+NJ+CT+RI+MA+VT+NH+ME	1.95	0.75	0.38	0.40
NM	1.36	0.84	0.77	0.78
NV	4.07	3.33	3.30	3.30
OFFSHR	1.00	1.00	1.00	1.00
OH	3.48	1.45	1.06	1.09
OK	1.92	0.95	0.84	0.85
PA	0.65	0.23	0.13	0.13
SD-MN-WI	0.63	0.41	0.38	0.38
TN+GA+NC+SC	0.28	0.06	0.06	0.06
TXG	0.90	0.47	0.44	0.44
TXN	0.90	0.47	0.44	0.44
TXW	1.88	1.12	1.07	1.07
UT	0.95	0.37	0.30	0.31

VA+MD+DE	1.29	0.53	0.24	0.26
WV	0.50	0.19	0.11	0.12
WY	2.59	1.34	1.21	1.23

[1]Texas Gulf and Texas Central VOC emissions were based on estimates of VOC emissions in the Gulf Coast NEMS region within Texas. The proportion of those emissions allocated to the Texas Gulf tag versus the Texas Central tag is based on the relative VOC emissions magnitudes within each of the 2026 tags such that 72.4% of the VOC emissions from the Gulf Coast NEMS were allocated to the Texas Gulf tag and 27.6% of the VOC emissions from the Gulf Coast NEMS were allocated to the Texas Central Tag.

[2]VOC emissions in the Texas West region is the sum of estimated VOC emissions in the Texas Midcontinent NEMS region and the Texas Southwest NEMS region.

Table 3-7. 2038 year ozone scaling factors for oil and natural gas tags in the baseline and regulatory alternatives based on ratios of VOC emissions in those scenarios to the 2026 modeled scenario for each state-by-state oil and natural gas tag.

State	Baseline	Less Stringent Alternative	More Stringent Alternative	Final Rule
AL	0.92	0.30	0.19	0.20
AR	3.27	0.88	0.56	0.59
AZ	1.34	0.34	0.32	0.32
CA	1.58	1.54	1.50	1.50
CO	1.84	1.84	1.77	1.78
FL	0.59	0.24	0.21	0.21
IL	0.01	0.00	0.00	0.00
IN	0.04	0.01	0.01	0.01
KS	0.96	0.38	0.25	0.26
KY	0.41	0.15	0.08	0.09
LA	1.35	0.41	0.32	0.32
MI	0.65	0.28	0.16	0.17
MO	0.18	0.07	0.06	0.06
MS	1.94	0.84	0.77	0.77
MT+ID+WA+OR	0.78	0.39	0.33	0.33
ND	3.19	2.20	2.17	2.17
NE+IA	1.50	0.58	0.47	0.47
NY+NJ+CT+RI+MA+VT+NH+ME	1.53	0.57	0.32	0.34
NM	1.44	0.86	0.80	0.81
NV	1.33	0.81	0.79	0.79
OFFSHR	1.00	1.00	1.00	1.00
OH	3.35	1.31	1.06	1.08
OK	2.16	0.92	0.82	0.83
PA	0.63	0.19	0.12	0.12
SD-MN-WI	0.41	0.20	0.17	0.17
TN+GA+NC+SC	0.29	0.07	0.07	0.07

TXG	1.01	0.51	0.49	0.49
TXN	1.01	0.51	0.49	0.49
TXW	2.08	1.12	1.08	1.08
UT	0.81	0.26	0.19	0.20
VA+MD+DE	1.21	0.50	0.23	0.25
WV	0.46	0.16	0.11	0.11
WY	2.50	1.02	0.92	0.93

[1]Texas Gulf and Texas Central VOC emissions were based on estimates of VOC emissions in the Gulf Coast NEMS region within Texas. The proportion of those emissions allocated to the Texas Gulf tag versus the Texas Central tag is based on the relative VOC emissions magnitudes within each of the 2026 tags such that 72.4% of the VOC emissions from the Gulf Coast NEMS were allocated to the Texas Gulf tag and 27.6% of the VOC emissions from the Gulf Coast NEMS were allocated to the Texas Central Tag.

[2]VOC emissions in the Texas West region is the sum of estimated VOC emissions in the Texas Midcontinent NEMS region and the Texas Southwest NEMS region.

4. Evaluation of CAMx Model Ozone Predictions Against Ambient Ozone Measurements in 2016

An operational model evaluation was conducted for the 2016 base year CAMx v7.10 simulation performed for the 12 km U.S. modeling domain. The purpose of this evaluation is to examine the ability of the 2016 air quality modeling platform to represent the magnitude and spatial and temporal variability of measured (i.e., observed) maximum daily average (i.e., MDA8) ozone concentrations within the modeling domain. Reasonable model performance in 2016 builds confidence the credibility of using this modeling platform to project ozone to the 2026 timeframe. The evaluation presented here is based on model simulations using the 2016v2 emissions platform (i.e., scenario name 2016fj). The model evaluation for ozone focuses on comparisons of 8-hour daily maximum (i.e., MDA8) ozone concentrations to the corresponding observed data at monitoring sites in the EPA Air Quality System (AQS). The locations of the ozone monitoring sites in this network are shown in Figure 4-1.

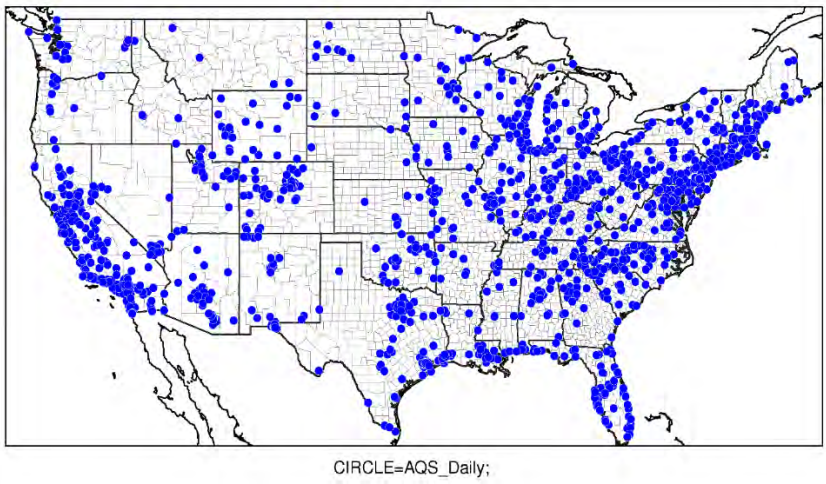

Figure 4-1. Location of ozone monitoring sites.

This evaluation includes statistical measures and graphical displays of model performance based upon model-predicted versus observed concentrations. The evaluation focuses on model predicted and observed MDA8 ozone concentrations that were paired in space and time. Model performance statistics were calculated for several spatial scales for the April-September 2016 time period. Statistics were calculated in aggregate for monitoring sites within each of nine climate regions of the 12 km U.S. modeling domain as well as nationally. The regions include the Northeast, Ohio Valley, Upper Midwest, Southeast, South, Southwest, Northern Rockies & Plains, Northwest, and West[20], which are defined based upon the states[21] contained within the National Oceanic and Atmospheric Administration (NOAA) climate regions (Figure 4-2)[22] as defined in Karl and Koss (1984).

[20] Note most monitoring sites in the West region are located in California (see Figures A-1 and A-2), therefore the statistics for the West region will be mostly representative of model performance in California ozone.

[21] The nine climate regions are defined by States where: Northeast includes CT, DE, ME, MA, MD, NH, NJ, NY, PA, RI, and VT; Ohio Valley includes IL, IN, KY, MO, OH, TN, and WV; Upper Midwest includes IA, MI, MN, and WI; Southeast includes AL, FL, GA, NC, SC, and VA; South includes AR, KS, LA, MS, OK, and TX; Southwest includes AZ, CO, NM, and UT; Northern Rockies & Plains includes MT, NE, ND, SD, WY; Northwest includes ID, OR, and WA; and West includes CA and NV.

[22] NOAA, National Centers for Environmental Information scientists have identified nine climatically consistent regions within the contiguous U.S., http://www.ncdc.noaa.gov/monitoring-references/maps/us-climate-regions.php.

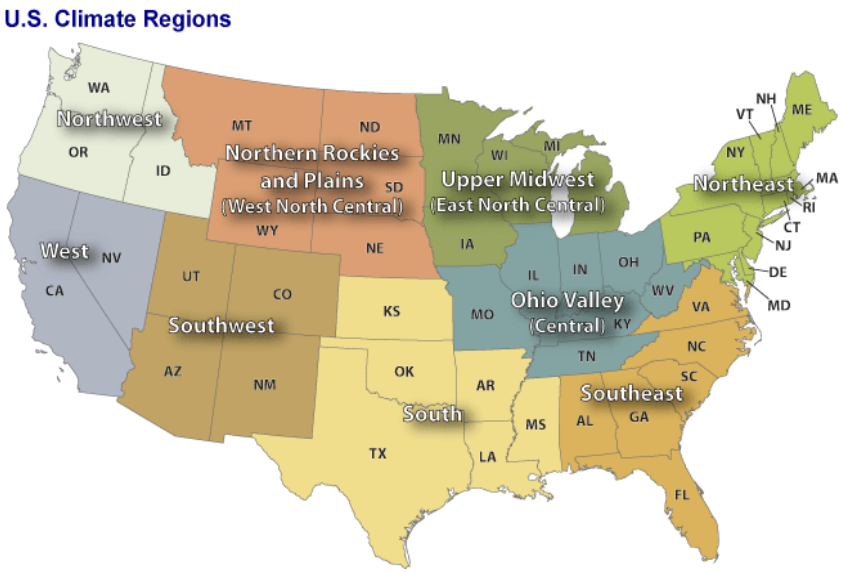

Figure 4-2. NOAA climate regions **(source: http://www.ncdc.noaa.gov/monitoring-references/maps/us-climate-regions.php#references)**

Statistics were created using data on all April-September days with valid observed data during this period. In addition, this section provides maps that show the mean bias and normalized mean bias for April through September at individual monitoring sites and time series plots (April through September) of observed and predicted MDA8 ozone concentrations for each region. The Atmospheric Model Evaluation Tool (AMET) was used to calculate the model performance statistics used in this document (Gilliam et al., 2005). For this evaluation we have selected the mean bias, mean error, normalized mean bias, normalized mean error and correlation to characterize model performance, statistics which are consistent with the recommendations in Simon et al. (2012) and EPA's photochemical modeling guidance (U.S. EPA, 2018). For formulas listed below, P represents CAMx predicted MDA8 ozone, O represents observed MDA8 ozone and n represents the number of model-observation data pairs

- Mean bias (MB) is the average of the difference (predicted – observed) divided by the total number of replicates. Mean bias is given in units of ppb and is defined as:

$$MB = \frac{1}{n}\sum_{1}^{n}(P - O)$$

- Mean error (ME) calculates the absolute value of the difference (predicted - observed) divided by the total number of replicates. Mean error is given in units of ppb and is defined as:

$$ME = \frac{1}{n}\sum_{1}^{n}|P - O|$$

- Normalized mean bias (NMB) is the average the difference (predicted - observed) over the sum of observed values. NMB is a useful model performance indicator because it avoids over inflating the observed range of values, especially at low concentrations. Normalized mean bias is given in percentage units and is defined as:

$$NMB = \frac{\sum_1^n (P - O)}{\sum_1^n (O)} * 100$$

- Normalized mean error (NME) is the absolute value of the difference (predicted - observed) over the sum of observed values. Normalized mean error is given in percentage units and is defined as:

$$NME = \frac{\sum_1^n |P - O|}{\sum_1^n (O)} * 100$$

- Correlation (r) is a measure of the ability of the model to capture spatial and temporal variation in the observations. Correlation values range from -1 to +1. A correlation of +1 represents a perfect linear correlation between the observations and the model values and a correlation of -1 represents perfectly anticorrelated datasets. A correlation value of 0 would represent datasets whose relationship is completely random. Correlation is calculated as:

$$r = \frac{\sum(O_i - \bar{O}) \times (P_i - \bar{P})}{\sqrt{\sum(O_i - \bar{O})^2 \sum(P_i - \bar{P})^2}}$$

As described in more detail below, the model performance statistics indicate that the MDA8 ozone concentrations predicted by the 2016v2 CAMx modeling platform closely reflect the corresponding MDA8 observed ozone concentrations in each region of the 12 km US modeling domain. The acceptability of model performance was judged by considering the 2016v2 CAMx performance results in light of the range of performance found in recent regional ozone model applications (Emery et al., 2017; NRC, 2002; Phillips et al., 2007; Simon et al., 2012; U.S. EPA, 2005; U.S. EPA, 2009; U.S. EPA, 2010). These other modeling studies represent a wide range of modeling analyses that cover various models, model configurations, domains, years and/or episodes, chemical mechanisms, and aerosol modules. In particular, Emery et.al. extend the results of Simon et.al., to include performance results from a few more recent photochemical model applications. The results in the former paper indicate that about a third of the top performing past applications have normalized mean bias and a normalized mean error statistics for MDA8 ozone of less than ±5 percent and less 15 percent, respectively. In addition, two-thirds of past applications have normalized mean bias less than ±15 percent and normalized mean error less than 25 percent. These "criteria" are not intended to represent "rigid pass/fail tests" but rather as "simple references to the range of recent

historical performance" that can be used to understand where the performance results of a particular application "fall in the spectrum of past published results."

Overall, the ozone model performance results for the 2016v2 CAMx simulation are generally within the range found in other recent peer-reviewed and regulatory applications. The model performance results, as described in this document, demonstrate that the predictions from the 2016v2 modeling platform correspond closely to observed concentrations in terms of the magnitude, temporal fluctuations, and geographic differences for MDA8 ozone concentrations.

The MDA8 ozone model performance bias and error statistics for the period April-September for each climate region are provided in Table 4-1. The model performance statistics provided in Table 4-1 show that regional mean bias is less than ±5 ppb[23] and the mean error is between 6 and 7.5 ppb during the April through September in each region. Normalized mean bias is less than ± 5% in the Northeast, Ohio Valley, Southeast, South, and Northwest as well as nationally. In the Upper Midwest, Southwest, Northern Rockies & Plains, and West, normalized mean bias is between 7% and 10%. Normalized mean error is less than 15% in the Ohio Valley, Southeast, Northern Rockies & Plains, Southwest and West and less than 20% in the other regions. Correlation was between 0.7 and 0.8 for all regions except for the Southwest and Northwest where correlation was 0.62 and 0.67 respectively.

Table 4-1. Model Performance Statistics for April-September MDA8 O_3 at AQS monitors

Region	MB	NMB	ME	NME	Cor
Northeast	-1.3	-2.8	6.8	15.3	0.77
Ohio Valley	-0.5	-1.1	6.4	14.1	0.73
Upper Midwest	-3.9	-9.3	6.8	16.3	0.75
Southeast	0.9	2.1	6.0	14.2	0.81
South	-0.6	-1.5	6.6	16.1	0.73
Northern Rockies & Plains	-4.1	-9.4	6.4	14.7	0.71
Southwest	-4.4	-8.4	7.0	13.6	0.62
Northwest	-0.3	-0.7	6.6	17.7	0.67
West	-3.5	-6.9	7.4	14.5	0.80
National	-1.7	-3.8	6.7	14.8	0.77

Spatial plots of the April-September MDA8 ozone mean bias and normalized mean bias and error at individual monitors nationwide are shown in Figures 4-3 and 4-4. Mean bias, as seen in Figure 4-3, is within ± 5 ppb at many sites from portions of Texas northeastward to the Northeast Corridor. At monitors in this area the normalized mean bias is generally within ± 10 percent. At most

[23] Note that "within ±5 ppb" includes values that are greater than or equal to -5 ppb and less than or equal to 5 ppb.

monitoring sites across the remainder of the East the model under predicts by 5 to 10 ppb, the normalized mean bias is between -10 and -20 percent. In Arizona, Colorado, New Mexico, and Utah, there is notable spatial heterogeneity in mean bias. For example, in Denver there are some sites with mean bias within ± 2 ppb while at relatively near-by monitors the model is low-biased by 5 to 10 ppb. In California, the model overpredicts April through September MDA8 ozone at coastal sites by 2-8 ppb and underpredicts April through September MDA8 in the central valley by 10-20 ppb. For most monitoring sites in the West, the normalized mean bias is -20 percent or less, except for central California where the normalized mean bias is between -20 and -30 percent.

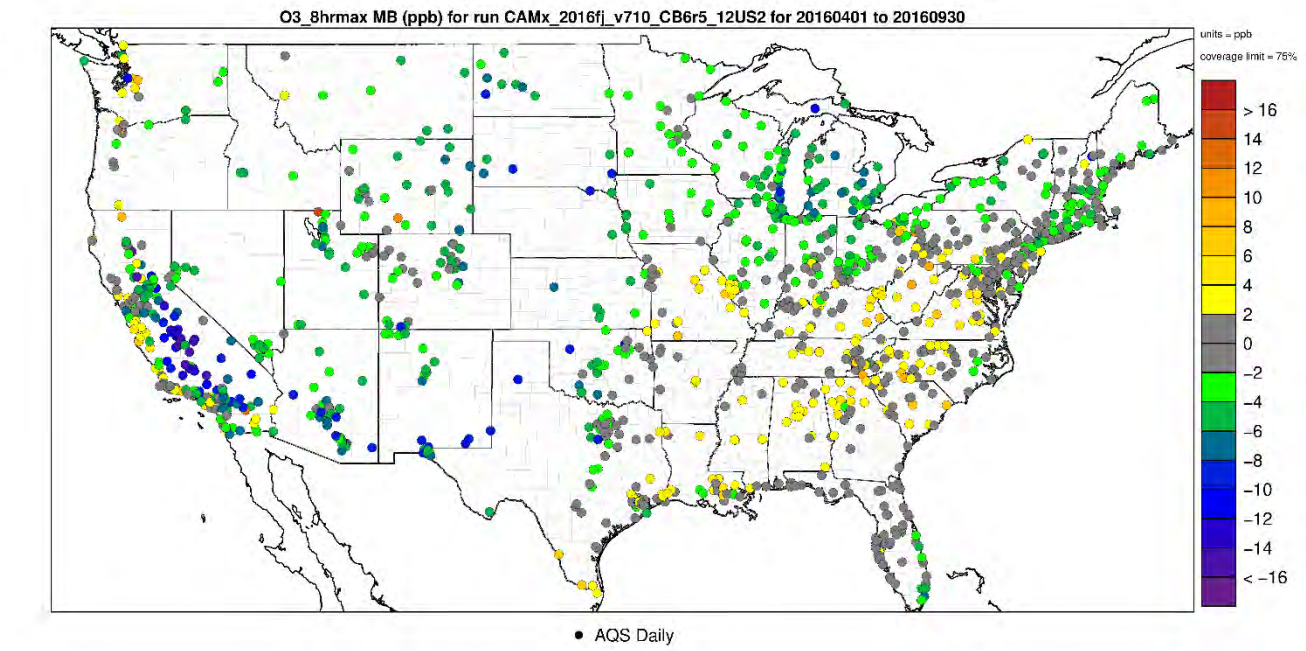

Figure 4-3. Map of April-September Mean Bias (ppb) for MDA8 ozone at AQS monitoring locations

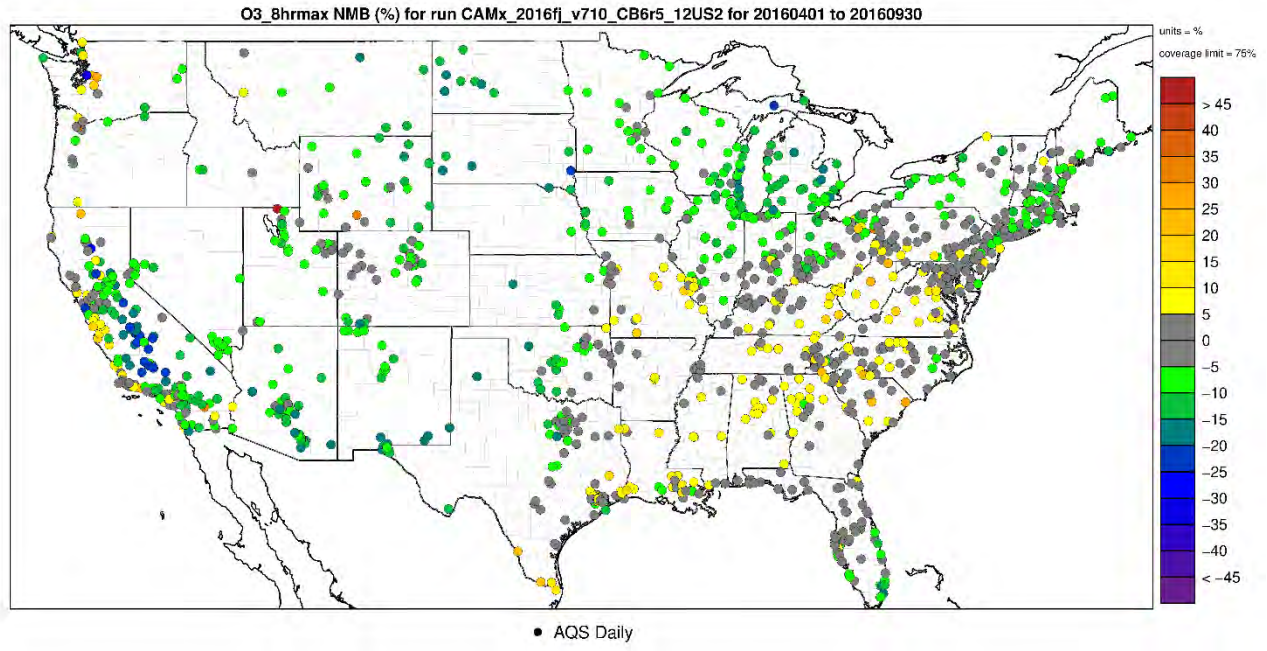

Figure 4-4. Map of April-September Normalized Mean Bias (%) for MDA8 ozone at AQS monitoring locations

Time series plots of observed and predicted MDA8 ozone during April through September 2016 for each region and are provided in Figures 4-5 through 4-7 respectively. The plots in this figure show that the modeled concentrations closely track the corresponding observed values in terms of day-to-day fluctuations and the general magnitude of concentrations. Comparing the plots for the nine regions reveals that there are large differences in the day-to-day variability among the regions. For example, the degree of temporal variability in MDA8 ozone concentrations in the Northeast, Upper Midwest, and Ohio Valley is much greater than in the Southeast, South, Southwest, and Northern Rockies & Plains. The modeling platform captures regional differences in the degree of temporal variability in MDA8 ozone concentrations. The model performs equally as well in eastern and western regions in terms of replicating the relative magnitude of concentrations and day-to-day variability that are characteristic of observed MDA8 ozone concentrations in each region.

There are some differences in the model performance noticeable throughout different portions of the April through September time period. In the Northeast and the Ohio Valley, the model underpredicts in April, May, and June followed by over prediction July. In the Upper Midwest, the observed concentrations are underpredicted in April, May and June, MDA8 values of the model generally align with the corresponding observed data in July, August, and September. In the

Southeast, the predictions generally correspond well with that of the observed concentrations in April, May and June with overprediction during the remainder of the ozone season. In the South, the predicted concentrations tend to be close to that of the observed data in most months with a tendency for underprediction of peak values in April and May. In the Southwest, the modeled values are underpredicted in the early part of the season but align better with observations in August and September. In the Northern Rockies and Plains, the model underpredicts in April through July, but closely captures the distribution of observed concentrations in August and September. In the Northwest modeled MDA8 ozone underpredicts the observed values in April through June, but then more closely tracks the observed values in July, August, and September. In the West region, the observed ozone is underpredicted in April through September with a tendency to under predict peak values.

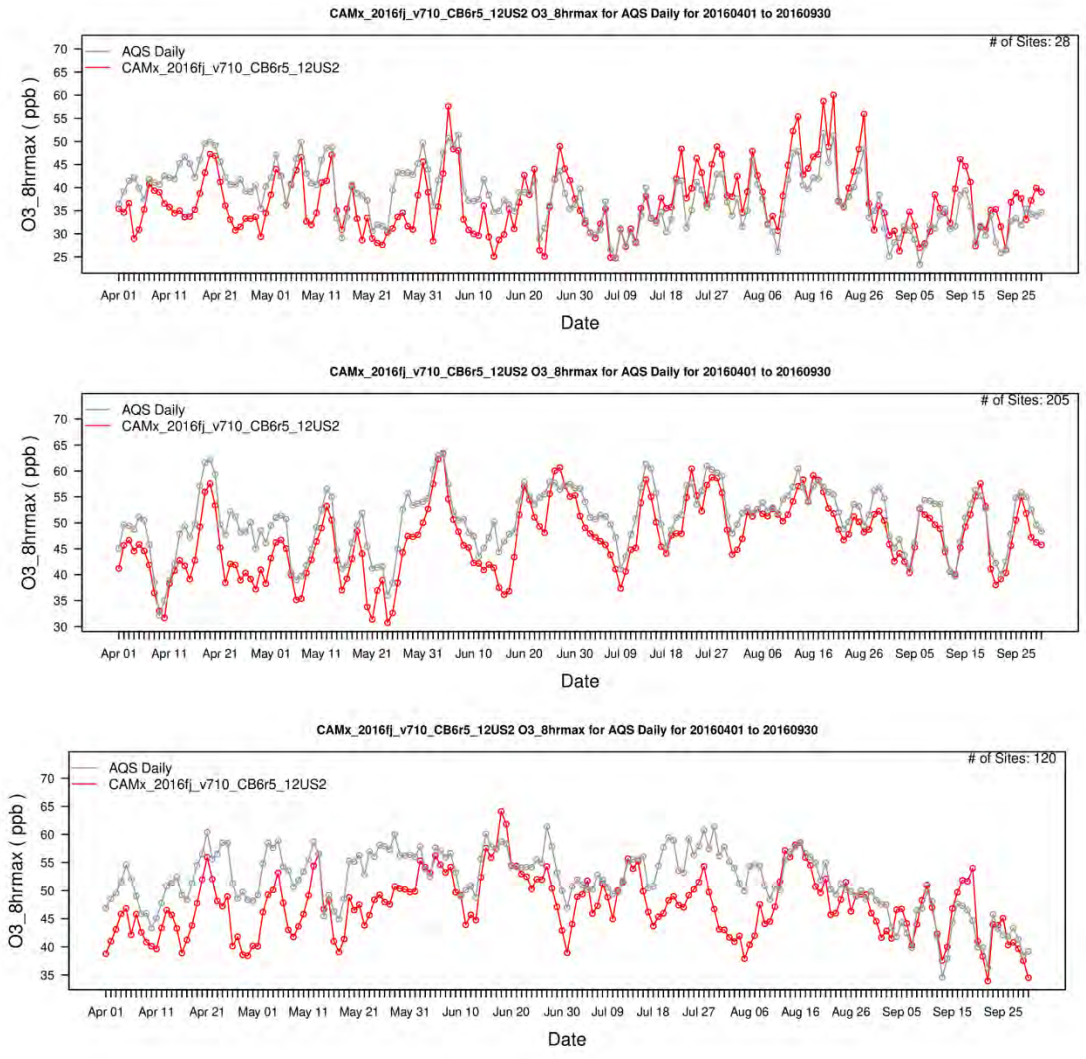

Figure 4-5. Timeseries of observed and modeled daily MDA8 ozone (ppb) from April to September averaged across monitors in the Northwest (top), West (middle), and Southwest (bottom).

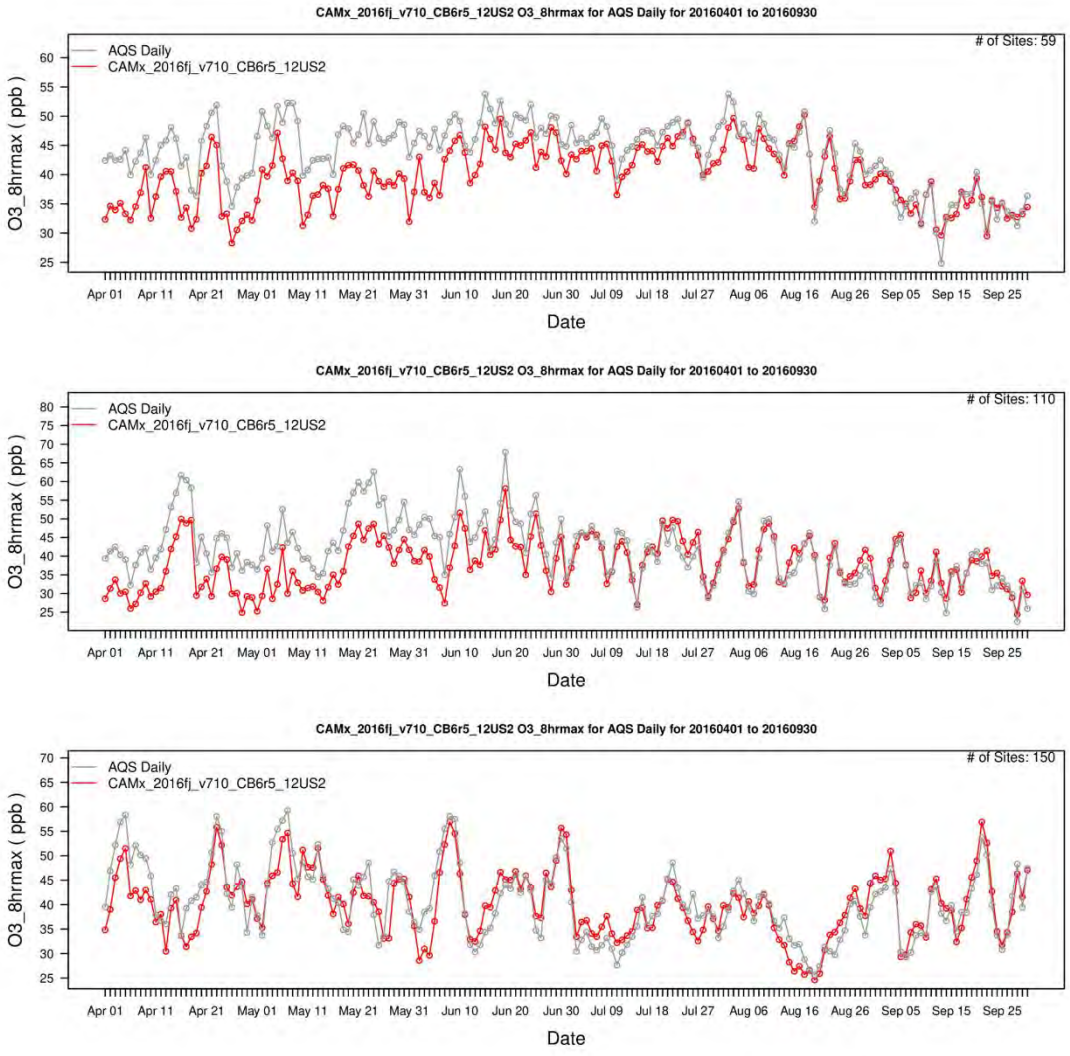

Figure 4-6. Timeseries of observed and modeled daily MDA8 ozone (ppb) from April to September averaged across monitors in the Northern Rockies & Plains (top), Upper Midwest (middle), and South (bottom).

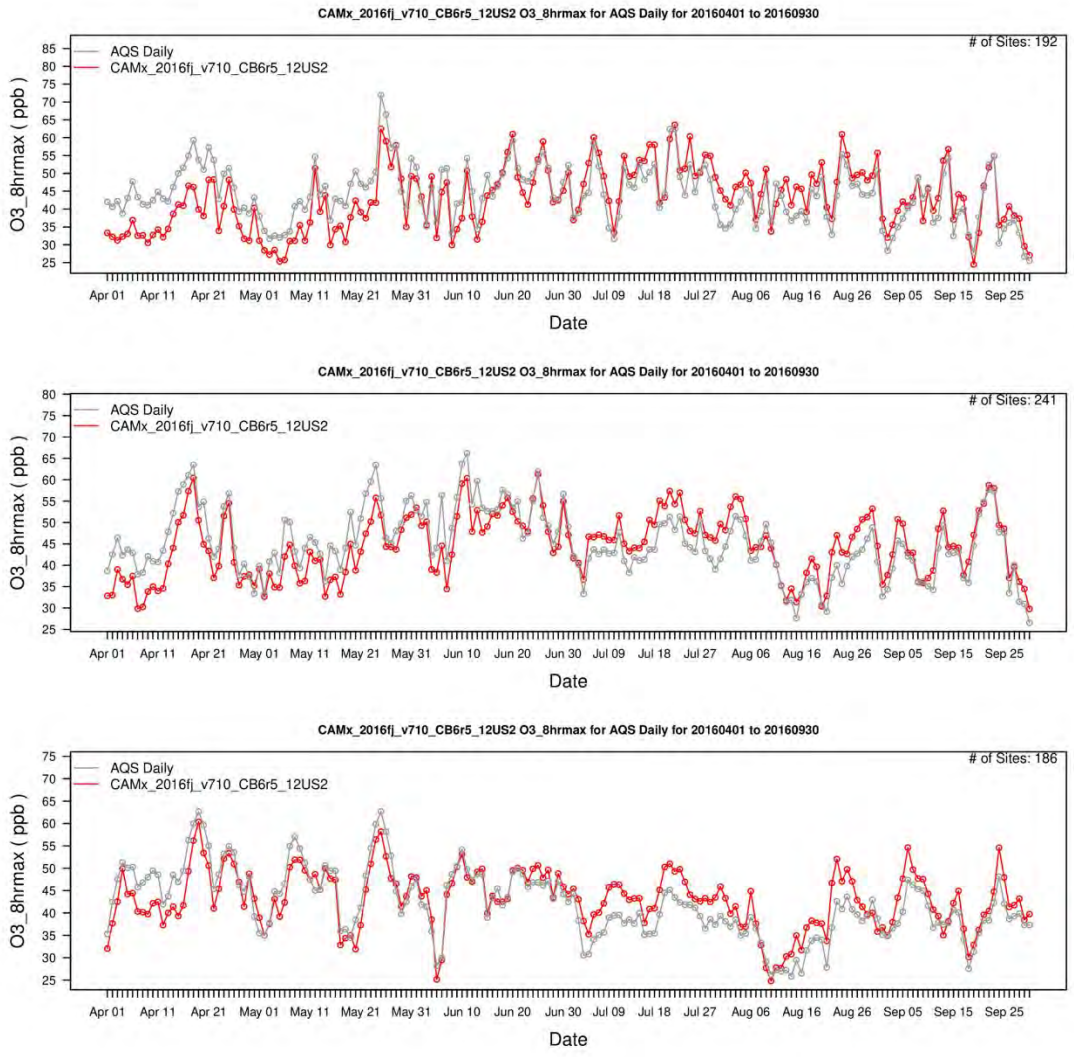

Figure 4-7. Timeseries of observed and modeled daily MDA8 ozone (ppb) from April to September averaged across monitors in the Northeast (top), Ohio River Valley (middle), and Southeast (bottom).

In summary, the ozone model performance statistics for the CAMx 2016fj (2016v2) simulation are within or close to the ranges found in other recent peer-reviewed applications (e.g., Simon et al, 2012 and Emery et al, 2017). The predictions from the 2016v2 modeling platform generally correspond closely to observed concentrations in terms of the magnitude, temporal fluctuations, and geographic differences for MDA8 ozone concentrations. Thus, the model performance results demonstrate the scientific credibility of our 2016v2 modeling platform. These results provide confidence in the ability of the modeling platform to provide a credible basis for use in estimating future year benefits associated with this rule.

5. Evaluation of Methods for Estimating Ozone Impacts based on Oil & Gas Source Apportionment Modeling using Two Emissions Sensitivity Scenarios

The methods described in section 4 have been used for previous EPA rulemakings focusing on electric generating units (EGUs) (U.S. EPA, 2019b, 2020a, 2020b, 2021, 2023a, 2023b, 2023c, 2023d) and were developed to address the challenge of rapidly generating spatially resolved air quality impacts to support EPA rulemakings whose schedules do not allow the time necessary to simulate the final regulatory alternatives using full photochemical air quality modeling simulations. The purpose of this analysis is to provide further information on the accuracy of the methods used to estimate ozone impacts in this rulemaking by comparing estimates of ozone impacts derived from these methods against results to those that would be obtained from a photochemical modeling simulation. Specifically, we provide comparisons of results for emissions scenarios focusing on the oil and natural gas sector, while previous applications have analyzed emissions scenarios for the EGU sector.

As described below, we construct two hypothetical oil and natural gas emissions scenarios with which to demonstrate the capabilities for the state-level oil and natural gas source apportionment dataset and methods describe in Section 4. Note that these hypothetical emissions scenarios are not regulatory alternatives but rather emissions perturbations that were designed for the purpose of testing the ozone changes that would result from changes in emissions from the oil and natural gas sector. Ozone impacts for these two hypothetical emissions scenarios were simulated with the CAMx model and serve as a basis against which to compare impacts derived using the source apportionment scaling methodology described in Section 4 with state-by-state oil and natural gas emissions tags.

The steps for comparing the source apportionment scaling methodology to CAMx model results are as follows:

1. Create gridded 12 km ozone impacts using the CAMx model
    1.1. Simulate the 2026fj base case emissions using the CAMx Model
    1.2. Simulate the hypothetical emissions cases using the CAMx Model
    1.3. Create gridded eVNA surfaces of AS-MO3 for model simulations in steps 1.1 and 1.2 using eq 1 from Section 3.2
    1.4. Using the gridded eVNA surfaces, create gridded 12 km ozone impacts for each of the hypothetical emissions scenarios compared to the 2026fj base case

2. Create eVNA gridded 12km ozone impacts using the source apportionment scaling method described in Section 3.2 for the hypothetical emissions cases.
   2.1. Subtract surfaces of the 2026fj basecase from each hypothetical emissions case to create gridded surfaces of ozone impacts for each emissions case.
3. Compare gridded ozone impacts from step 1 and step 2, using the CAMx simulations as the benchmark

The first hypothetical oil and natural gas emissions scenario was a 35% across-the-board reduction in the 2026fj sector-wide VOC emissions. The emissions reductions were simulated for the entire sector as defined in the 2016v2 EPA emissions modeling platform (US EPA, 2022a) and includes both sources that are regulated under this rulemaking and sources that are not regulated under this rulemaking. The second hypothetical emissions scenario involved replacing 2026 oil and natural gas projected NOx and VOC emission with 2023 projections from the v2 version of EPA's 2016 emissions platform (US EPA, 2022a). VOC emissions changes in these scenarios compared to the 2026fj base case are provided in Table 5-1. Because the source apportionment tags described in Section 4 tracked emissions from SCCs expected to be impacted by this rulemaking there is a mismatch between the emissions tagged in the source apportionment modeling and the emissions sources impacted in the 35% VOC cut hypothetical emissions scenario. In states where the magnitude of VOC emissions reductions for this scenario (Table 5-1) are larger than the total emissions tracked for the state (Table 3-3), the source apportionment scaling methodology using the dataset designed for this rulemaking cannot be used to simulate the full impact of the 35% across-the-board VOC cut.

Table 5-1. Emissions changes for two hypothetical oil and natural gas emissions scenarios in relation to the 2026fj base case

State	Emissions changes for the 35% O&G VOC emissions cut scenario (tpy)		Emissions changes for the 2023 O&G emissions scenario (tpy)	
	NOx	VOC	NOx	VOC
Alabama	0	-3,844	104	76
Arizona	0	-133	-9	-7
Arkansas	0	-2,013	191	278
California	0	-2,128	505	1,046
Colorado	0	-27,303	332	0
Florida	0	-455	-268	-43
ID+MT+OR	0	-10,363	17	-10
Illinois	0	-19,080	-85	-153
Indiana	0	-3,907	-171	-33

Kansas	0	-26,844	821	1,608
Kentucky	0	-12,348	317	-36
Louisiana	0	-27,968	69	-3,436
MD+VA	0	-2,570	81	64
Michigan	0	-5,578	257	-33
Mississippi	0	-3,584	26	-55
Missouri	0	-404	-319	-25
IA+NE	0	-1,031	-595	-57
Nevada	0	-74	2	0
NJ+NY	0	-2,102	-57	-85
New Mexico	0	-80,177	140	0
North Dakota	0	-109,431	663	0
Ohio	0	-6,558	-229	-989
Oklahoma	0	-72,020	4,554	10,013
Pennsylvania	0	-47,931	-644	-6,523
SC+TN	0	-1,036	-424	-108
SD+MN+WI	0	-1,858	-236	-55
Texas Central	0	-52,662	2,017	926
Texas Gulf	0	-132,985	2,473	-5,727
Texas West	0	-174,978	-260	-23,548
Utah	0	-24,062	29	0
West Virginia	0	-49,888	-1,114	-8,154
Wyoming	0	-24,144	33	0
Offshore	0	-16,910	0	0
US Total	0	-946,371	8,219	-35,066

Table 5-2 and Figure 5-1 compare ozone concentrations changes estimated using the source apportionment scaling approach to those simulated with the CAMx photochemical model for the 35% oil and natural gas sector VOC cut emissions scenario. Source apportionment scaling ozone impacts matched CAMx ozone impacts very well except in locations with very small impacts (the Northwest and West climate regions both had average ozone impacts less than 0.001 ppb as predicted by CAMx). For all other climate regions, normalized mean bias was at or below ±26% and correlation coefficients were in the range of 0.76-0.98. When calculated for the US as a whole, the normalized mean bias of ozone impacts was 16% and the correlation coefficient was 0.96. This indicates that overall, the source apportionment scaling methodology slightly underestimate the magnitude of the CAMx ozone impacts but generally replicates the spatial nature of these impacts for this emissions scenario.

Some of the locations visible in Figure 5-2 where the source apportionment scaling method underestimates the CAMx ozone impacts are due to the emissions mismatch described above between

the source apportionment tags and the emissions reductions for this scenario. For instance, only 72,735 tons per year of North Dakota oil and natural gas VOC emissions were tracked in the South Dakota source apportionment modeling tag but 109,431 tpy of VOC reductions were simulated through CMAx from North Dakota in the hypothetical emissions scenario. Similarly, the source apportionment tag for offshore oil and natural gas sources included 12,274 tpy of VOC emissions but the hypothetical emissions scenario reduced offshore oil and natural gas VOC emissions by 16,910. The darker green shades in North Dakota and in the Gulf of Mexico are therefore due to the fact that the emissions scaling method only accounted for 66% and 73% of the VOC emissions reductions modeled by CAMx in those locations. Even so, the mean bias of predicted ozone impacts for the Northern Rockies and Plains climate region is only 25.8%.

Table 5-2. Comparison of ozone impacts estimated from source apportionment scaling versus CAMx for hypothetical emissions scenario with 35% VOC cuts across all oil and natural gas sources. In regions with ozone reductions predicted by CAMx (shown as negative changes), a negative bias indicates the SA scaling method overpredicts impacts and a positive bias indicates the SA scaling method underpredicts impacts.

Region	Change in O3 from Emissions Sensitivity (ppb)		MB (ppb)	NMB (%)	Correlation Coefficient (r)
	SA scaling	CAMx			
Northeast	-0.012	-0.014	0.002	13.2	0.98
Northern Rockies & Plains	-0.019	-0.025	0.007	25.8	0.90
Northwest	-0.001	0.001	-0.002	-273.5	-0.09
Ohio Valley	-0.024	-0.027	0.004	13.0	0.93
South	-0.037	-0.046	0.009	19.3	0.97
Southeast	-0.007	-0.006	-0.001	-14.4	0.76
Southwest	-0.022	-0.024	0.002	7.3	0.98
Upper Midwest	-0.017	-0.022	0.005	24.2	0.98
West	-0.001	-2.6E-05	-0.001	-5552.6	0.35
US	-0.018	-0.022	0.004	16.0	0.96

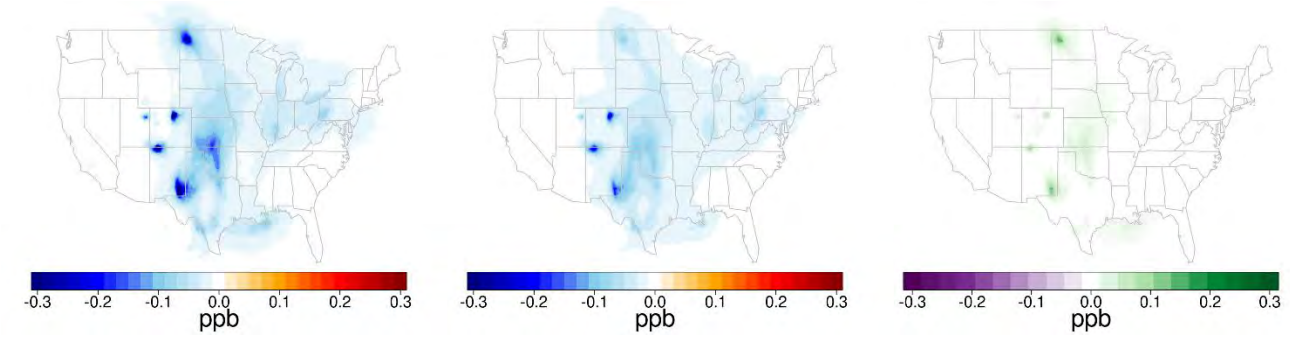

Figure 5-1. Maps comparing of ozone impacts estimated from CAMx (left) to estimates based on source apportionment scaling (center) for the hypothetical emissions scenario with 35% VOC cuts across all oil and natural gas sources. Absolute ozone differences between CAMx estimates and source apportionment scaling estimates are shown on the right panel.

For the second hypothetical emissions scenario involved replacing 2026 oil and natural gas projected NOx and VOC emission with 2023 projections, Table 5-1 shows that NOx emissions were projected to be higher in 2023 than in 2026 (by about 8,000 tpy) but VOC emissions were projected to be lower in 2023 than in 2026 (by over 35,000 tpy). As shown in Figure 5-2, these emissions changes resulted in spatially heterogeneous changes in CAMx ozone predictions with increases modeled in California and parts of the central US but decreases in ozone modeled near the Texas-New Mexico border and in the Northeastern US. Because the SCCs tagged in the source apportionment modeling did not include many of the oil and natural gas NO_x sources, the source apportionment scaling method was only partially able to replicate this scenario. NOx impacts on ozone were not quantified for any states where tagged NO_x emissions were less than 100 tpy and therefore the source apportionment scaling methodology did not capture an ozone impacts from NO_x changes in states other than Colorado, New Mexico, North Dakota, Oklahoma, Pennsylvania, Texas, West Virginia, and Wyoming. Specifically, there were 3 states without sufficient tagged NO_x emissions to scale which had NO_x emissions changes larger than 500 tpy in this emissions scenario: California, Kansas and New Jersey. In West Virginia, the total NOx decreases in the 2023 projections versus the 2026 projections were larger than the total tagged NOx emissions for that state. VOC tags were sufficient to fully capture simulated VOC emissions change in all states with the source apportionment scaling methodology. Ozone impacts were similar across the US with a normalized mean bias of 24.9% and a spatial correlation of 0.82. Ozone impacts in the regions with the largest CAMx-predicted ozone impacts were generally captured by the source apportionment scaling methodology as shown by statistics in Table 5-3 for the South, Northern Rockies and Plains and Northeast regions. Additionally Figure 5-2 shows similar bands of ozone increases in this scenario across Texas, Oklahoma and Northward as well as decreases in ozone in Western Pennsylvania. The source apportionment scaling methodology misses the ozone increases predicted by CAMx in California, likely as a result of not having sufficient tagged NO_x emissions to scale in California. A larger magnitude of normalized mean bias is apparent in Table 5-3 for several regions with very small modeled ozone impacts: Southeast, Ohio Valley and Upper Midwest.

Table 5-3. Comparison of ozone impacts estimated from source apportionment scaling versus CAMx for hypothetical emissions scenario with 2023 oil and natural gas projections. In regions with ozone reductions predicted by CAMx (shown as negative changes), a negative bias indicates the SA scaling method overpredicts impacts and a positive bias indicates the SA scaling method underpredicts impacts.

Region	Change in O3 from Emissions Sensitivity (ppb)		MB (ppb)	NMB (%)	Correlation Coefficient (r)
	SA scaling	CAMx			
Northeast	-0.006	-0.007	0.001	19.9	0.69
Northern Rockies & Plains	0.010	0.007	0.003	52.3	0.92
Northwest	0.0003	0.0005	-0.0002	-31.6	0.23
Ohio Valley	0.003	0.001	0.003	533.9	0.80
South	0.033	0.031	0.002	6.7	0.77
Southeast	0.001	-0.003	0.004	133.5	0.38
Southwest	0.005	0.003	0.002	74.5	0.24
Upper Midwest	0.008	0.004	0.004	117.2	0.73
West	0.001	0.006	-0.006	-88.1	0.54
US	0.009	0.008	0.002	24.9	0.82

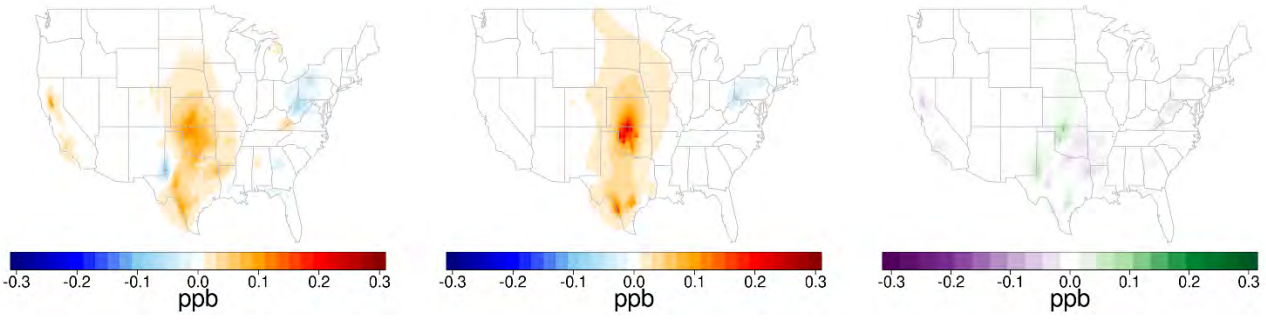

Figure 5-2. Maps comparing of ozone impacts estimated from CAMx (left) to estimates based on source apportionment scaling (center) for hypothetical emissions scenario with 2023 oil and natural gas emissions projections versus 2026 oil gas emissions projections. Absolute ozone

differences between CAMx estimates and source apportionment scaling estimates are shown on the right panel.

Overall, for these test cases using hypothetical emissions scenarios the source apportionment scaling methodology using the state-by-state oil and natural gas tags provided reasonable approximations of photochemical model-based ozone impacts. The largest discrepancies between the modeled impacts and the scaling method can be explained by discrepancies in how emissions were treated in the hypothetical case modeling and the source apportionment tags used in the scaling method. Since the source apportionment tags were designed explicitly to track the subset of sources impacted by this rulemaking those types of emissions discrepancies are not present in the rule analysis.

6. Uncertainties and Limitations of the Air Quality Methodology

One limitation of the scaling methodology for creating ozone surfaces associated with the baseline or regulatory alternatives described above is that the methodology treats ozone changes from the tagged sources as linear and additive. It therefore does not account for nonlinear atmospheric chemistry and does not account for interactions between emissions of different pollutants and between emissions from different tagged sources. The method applied in this analysis is consistent with how air quality impact analysis has been performed in several prior regulatory analyses U.S. EPA, 2019b, 2020a, 2020b, 2021, 2023a, 2023b, 2023c, 2023d).

We note that air quality is calculated in the same manner for the baseline and regulatory alternatives, so any uncertainties associated with these assumptions is propagated through results for both the baseline and regulatory alternatives in the same manner. While ozone formation often responds nonlinearly to changes in NO_X emissions, previous studies have shown that ozone concentrations generally respond more linearly to changes in VOC emissions (Hakami et al, 2003; Hakami et al., 2004). A second limitation is that the source apportionment contributions are informed by the spatial and temporal distribution of the emissions from each source tag as they occur in the 2026 modeled case. Thus, the contribution modeling results do not allow us to consider the effects of any changes to spatial distribution of oil and natural gas emissions within a state between the 2026 modeled case and the baseline and regulatory alternatives in this RIA. While oil and natural gas facilities may stop operating over time, new facilities are established. In general, in the timeframe of

the analysis for this rulemaking, new facilities are likely to be located in the same major basins as facilities that stop production. The analysis provided in Section 5 quantitatively assess the impacts for these two uncertainties and found that for the two hypothetical emissions cases analyzed, the combined effects of simplifying assumptions of linear scaling and static spatial distribution of emissions within the tagged sources resulted in mean biases of less than 25% compared to full-form CAMx modeling which accounted for the more complex treatment of chemistry and emissions changes. Finally, the 2026 CAMx-modeled concentrations themselves have some uncertainty. While all models have some level of inherent uncertainty in their formulation and inputs, the base-year 2016 model outputs have been evaluated against ambient measurements and have been shown to adequately reproduce spatially and temporally varying concentrations as described in section 4.

7. References

Ding, D., Zhu, Y., Jang, C., Lin, C.-J., Wang, S., Fu, J., . . . Qiu, X. (2016). Evaluation of health benefit using BenMAP-CE with an integrated scheme of model and monitor data during Guangzhou Asian Games. *Journal of Environmental Sciences*, **42**, 9-18. doi:https://doi.org/10.1016/j.jes.2015.06.003

Emery, C., Z. Liu, A. Russell, M. T. Odom, G. Yarwood, and N. Kumar, 2017. Recommendations on Statistics and Benchmarks to Assess Photochemical Model Performance. *J. Air and Waste Management Association*, **67**, 582-598.

Gilliam, R, W. Appel, and S. Phillips, 2005. The Atmospheric Model Evaluation Tool: Meteorology Module. Presented at the 4th Annual CMAS Conference, Chapel Hill, NC, September 2005. available at: http://www.cmascenter.org/conference/2005/abstracts/6_1.pdf

Gilliam, R.C. and J.E. Pleim, 2010. Performance Assessment of New Land Surface and Planetary Boundary Layer Physics in the WRF-ARW. *J. Appl. Meteor. Climatol.*, **49**, 760–774.

Gold, C. M., Remmele, P. R., & Roos, T. (1997). Voronoi methods in GIS. In M. van Kreveld, J. Nievergelt, T. Roos, & P. Widmayer (Eds.), Algorithmic Foundations of Geographic Information Systems (pp. 21-35). Berlin, Heidelberg: Springer Berlin Heidelberg.

Hakami, A., Odman, M.T., Russell, A.G., 2003. High-Order, Direct Sensitivity Analysis of Multidimensional Air Quality Models. *Environ. Sci. Technol*. **37**, 11, 2442-2452.

Hakami, A., Odman, M.T., Russell, A.G., 2004. Nonlinearity in atmospheric response: A direct sensitivity analysis approach. *Journal of Geophysical Research, Atmospheres*. **109**, D15303, doi:10.1029/2003JD004502.

Heath, N. K., Pleim, J.E., Gilliam, R., Kang, D., 2016. A simple lightning assimilation technique for improving retrospective WRF simulations. *Journal of Advances in Modeling Earth Systems.* **8**. 10.1002/2016MS000735

Hong, S. -Y., Noh, Y., & Dudhia, J. (2006). A new vertical diffusion package with an explicit treatment of entrainment processes. *Monthly Weather Review*, **134**, 2318-2341. doi:10.1175/MWR3199.1

Iacono, M.J., J.S. Delamere, E.J. Mlawer, M.W. Shephard, S.A Clough, and W.D. Collins, 2008. Radiative Forcing by Long-Lived Greenhouse Gases: Calculations with the AER Radiative Transfer Models, *J. Geophys. Res.,***113**, D13103.

Kain, J.S., 2004. The Kain-Fritsch Convective Parameterization: An Update, *J. Appl. Meteor.,* **43**, 170-181.

Karl, T.R. and Koss, W.J., 1984. Regional and National Monthly, Seasonal, and Annual Temperature Weighted by Area, 1895-1983. *Historical Climatology Series 4-3*, National Climatic Data Center, Asheville, NC, 38 pp.

Ma, L-M. and Tan Z-M, 2009. Improving the Behavior of Cumulus Parameterization for Tropical Cyclone Prediction: Convective Trigger, *Atmospheric Research*, **92**, 190-211.

Morrison, H.J., A. Curry, and V.I. Khvorostyanov, 2005. A New Double-Moment Microphysics Parameterization for Application in Cloud and Climate Models. Part I: Description, *J. Atmos. Sci.*, **62**, 1665–1677.

Morrison, H. and A. Gettelman, 2008. A New Two-Moment Bulk Stratiform Cloud Microphysics Scheme in the Community Atmosphere Model, version 3 (CAM3). Part I: Description and Numerical Tests, *J. Climate,* **21**, 3642-3659.

National Research Council (NRC), 2002. Estimating the Public Health Benefits of Proposed Air Pollution Regulations, Washington, DC: National Academies Press.

Phillips, S., K. Wang, C. Jang, N. Possiel, M. Strum, T. Fox, 2007. Evaluation of 2002 Multi-pollutant Platform: Air Toxics, Ozone, and Particulate Matter, 7th Annual CMAS Conference, Chapel Hill, NC, October 6-8, 2008. (http://www.cmascenter.org/conference/2008/agenda.cfm).

Pleim, J.E. and A. Xiu, 2003. Development of a Land-Surface Model. Part II: Data Assimilation, *J. Appl. Meteor.*, **42**, 1811–1822

Pleim, J.E., 2007a. A Combined Local and Nonlocal Closure Model for the Atmospheric Boundary Layer. Part I: Model Description and Testing, *J. Appl. Meteor. Climatol.*, **46**, 1383–1395.

Pleim, J.E., 2007b. A Combined Local and Nonlocal Closure Model for the Atmospheric Boundary Layer. Part II: Application and Evaluation in a Mesoscale Meteorological Model, *J. Appl. Meteor. Climatol.*, **46**, 1396–1409.

Ramboll Environ, 2021. User's Guide Comprehensive Air Quality Model with Extensions version 7.1, www.camx.com. Ramboll Environ International Corporation, Novato, CA.

Skamarock, W.C., J.B. Klemp, J. Dudhia, et al., 2008. A Description of the Advanced Research WRF Version 3. NCAR Tech. Note NCAR/TN-475+STR. http://wwww.mmm.ucar.edu/wrf/users/docs/arw_v3.pdf

Simon, H., K.R. Baker, and S.B. Phillips, 2012. Compilation and Interpretation of Photochemical Model Performance Statistics Published between 2006 and 2012, *Atmospheric Environment*, **61**, 124-139.

Stammer, D., F.J. Wentz, and C.L. Gentemann, 2003. Validation of Microwave Sea Surface Temperature Measurements for Climate Purposes, *J. of Climate*, **16(1)**, 73-87.

U.S. Environmental Protection Agency, 2005. Technical Support Document for the Final Clean Air Interstate Rule: Air Quality Modeling; Office of Air Quality Planning and Standards; Research Triangle Park, NC (CAIR Docket OAR-2005-0053-2149).

U.S. Environmental Protection Agency, 2007. Technical Report on Ozone Exposure, Risk, and Impact Assessments for Vegetation. Prepared by Abt Associates Inc. for U.S. Environmental

Protection Agency, Office of Air Quality Planning & Standards, Research Triangle Park, NC. EPA 452/R-07-002.

U.S. Environmental Protection Agency, 2009. Proposal to Designate an Emissions Control Area for Nitrogen Oxides, Sulfur Oxides, and Particulate Matter: Technical Support Document. Office of Air Quality Planning & Standards, Research Triangle Park, NC. EPA-420-R-007.

U.S. Environmental Protection Agency, 2010. Renewable Fuel Standard Program (RFS2) Regulatory Impact Analysis. Office of Transportation and Air Quality, Ann Arbor, MI. EPA-420-R-10-006.

U.S. Environmental Protection Agency, 2018. Modeling Guidance for Demonstrating Attainment of Air Quality Goals for Ozone, PM2.5, and Regional Haze. Office of Air Quality Planning & Standards, Research Triangle Park, NC. EPA 454/R-18-009.

U.S. Environmental Protection Agency, 2019a. Meteorological Model Performance for Annual 2016 Simulation WRF v3.8. Office of Air Quality Planning & Standards, Research Triangle Park, NC. EPA-454/R-19-010.

U.S. Environmental Protection Agency, 2019b. Regulatory Impact Analysis for the Repeal of the Clean Power Plan, and the Emission Guidelines for Greenhouse Gas Emissions from Existing Electric Utility Generating Units. Office of Air Quality Planning & Standards, Research Triangle Park, NC. EPA-452/R-19-003.

U.S. Environmental Protection Agency, 2020a. Analysis of Potential Costs and Benefits for the National Emission Standards for Hazardous Air Pollutants: Coal- and Oil-Fired Electric Utility Steam Generating Units – Subcategory of Certain Existing Electric Utility Steam Generating Units Firing Eastern Bituminous Coal Refuse for Emissions of Acid Gas Hazardous Air Pollutants. Office of Air Quality Planning & Standards, Research Triangle Park, NC. https://www.epa.gov/sites/default/files/2020-04/documents/mats_coal_refuse_cost benefit_memo.pdf

U.S. Environmental Protection Agency, 2020b. Benefit and Cost Analysis for Revisions to the Effluent Limitations Guidelines and Standards for the Steam Electric Power Generating Point Source Category. Office of Water, Washington D.C. EPA-821-R-20-003.

U.S. Environmental Protection Agency, 2021. Regulatory Impact Analysis for the Final Revised Cross-State Air Pollution Rule (CSAPR) Update for the 2008 Ozone NAAQS. Office of Air Quality Planning & Standards, Research Triangle Park, NC. EPA-452/R-21-002.

U.S. Environmental Protection Agency, 2022a. Technical Support Document (TSD): Preparation of Emissions Inventories for the 2016v2 North American Emissions Modeling Platform, Office of Air Quality Planning & Standards, Research Triangle Park, NC. EPA-454/B-22-001.

U.S. Environmental Protection Agency, 2022b. Software for Model Attainment Test - Community Edition (SMAT-CE) User's Guide Software version 2.1. Office of Air Quality Planning & Standards, Research Triangle Park, NC. EPA-454/B-22-013.

U.S. Environmental Protection Agency, 2023a. Benefit and Cost Analysis for Proposed Supplemental Effluent Limitations Guidelines and Standards for the Steam Electric Power Generating Point Source Category. Office of Water, Washington D.C. EPA-821-R-23-003.

U.S. Environmental Protection Agency, 2023b. Regulatory Impact Analysis for Final Federal Good Neighbor Plan Addressing Regional Ozone Transport for the 2015 Ozone National Ambient Air Quality Standard. Office of Air Quality Planning & Standards, Research Triangle Park, NC. EPA-452/R-23-001.

U.S. Environmental Protection Agency, 2023c Regulatory Impact Analysis for the Proposed National Emission Standards for Hazardous Air Pollutants: Coal- and Oil-Fired Electric Utility Steam Generating Units Review of the Residual Risk and Technology Review. Office of Air Quality Planning & Standards, Research Triangle Park, NC. EPA-452/R-23-002.

U.S. Environmental Protection Agency, 2023d Regulatory Impact Analysis for the Proposed New Source Performance Standards for Greenhouse Gas Emissions from New, Modified, and Reconstructed Fossil Fuel-Fired Electric Generating Units; Emission Guidelines for Greenhouse Gas Emissions from Existing Fossil Fuel-Fired Electric Generating Units; and Repeal of the Affordable Clean Energy Rule. Office of Air Quality Planning & Standards, Research Triangle Park, NC. EPA-452/R-23-006.

U.S. Environmental Protection Agency, 2023e Regulatory Impact Analysis of the Standards of Performance for New, Reconstructed, and Modified Sources and Emissions Guidelines for Existing Sources: Oil and Natural Gas Sector Climate Review. Office of Air Quality Planning & Standards, Research Triangle Park, NC. EPA-452/R-23-013.

Xiu, A., and J.E. Pleim, 2001, Development of a Land Surface Model. Part I: Application in a Meso scale Meteorological Model, *J. Appl. Meteor.,* 40, 192-209.

United States Environmental Protection Agency	Office of Air Quality Planning and Standards Air Quality Assessment Division Research Triangle Park, NC	Publication No. EPA-454/R-23-007 November 2023